universität wien

MASTERARBEIT

Titel der Masterarbeit

The function of the BRafV600E mutation in adult neural stem cells and paediatric malignant astrocytomas

Verfasser

Brian Reichholf, BSc

angestrebter akademischer Grad

Master of Science (MSc)

Wien, 2013

Studienkennzahl lt. Studienblatt:	A 066 834
Studienrichtung lt. Studienblatt:	Masterstudium Molekulare Biologie
Betreuerin:	Prof. Dr. Manuela Baccarini

Abstract

Malignant astrocytomas (MA) are aggressive brain tumours with generally poor prognosis. Grade IV astrocytomas, also known as glioblastoma multiforme (GBM), is one of the most aggressive gliomas. They are thought to arise from neural stem cells (NSCs), which undergo asymmetric cell division (ACD), resulting in two daughter cells of alternate fate, providing self-renewal through one and differentiation through the other. BRaf, a kinase involved in the MAPK pathway, has been found mutated or activated in ~4% of GBM, and the mutant $BRaf^{V600E}$ in combination with deletion of CDKN2A, encoding $p16^{Ink4a}$ and $p19^{Arf}$, has been found associated with paediatric MA. $BRaf^{V600E}$ is known to signal proliferation and differentiation, however it is unknown if transformation is associated with an increase in self-renewal and thus disruption of ACD.

In this thesis I make use cells isolated from a Cre-inducible $BRaf^{V600E}$ mouse model with concomitant Ink4a/Arf deletion. The following data shows, that expression of $BRaf^{V600E}$ leads to an increase in symmetric cell division in NSCs, an increase in proliferative capacity, and a decrease in differentiation potential. Furthermore, specifically inhibiting of $BRaf^{V600E}$ using the FDA-approved drug vemurafenib (PLX4032/PLX4720) shows a restoration of differentiation potential and a reduction in proliferation and self-renewing NSCs.

Zusammenfassung/Abstract

Bösartige Astrozytome (malignant astrocytoma, MA) sind aggressive Hirntumore mit allgemein schlechter Prognose. Nach WHO klassifizierte Grad IV Astrozytome, auch als glioblastoma multiforme (GBM) bekannt, sind eine der aggressivsten Gliome. Als Ursprung vermutet man neuralen Stammzellen (neral stem cells, NSCs), die im Normalfall asymmetrische Zellteilung (asymmetric cell division, ACD) betreiben, woraus sich die zwei Tochterzellen mit unterschiedlichem Differenzierungsschicksal bilden. Dies ermöglicht eine Selbsterneuerung der Stammzellpopulation in einer Tochterzelle und gleichzeitige Differenzierung in der anderen. BRAF, eine Kinase in dem MAPK Weg, ist in ~4% der GBM-Fälle entweder mutiert oder aktiviert. Die Mutante $BRAF^{V600E}$ in Kombination mit der Deletion des CDKN2A Lokus, der für die Tumorsuppressoren $p16^{Ink4a}$ und $p19^{Arf}$ kodiert, wird vorwiegend mit pädiatrischen MA assoziert. Es ist bekannt, dass $BRAF^{V600E}$ sowohl die Proliferation als auch Differenzierung signalisieren kann, aber es ist nicht klar, ob die Tumortransformation mit einem Anstieg der Selbsterneuerung und damit der Unterbrechung der ACD verbunden ist.

In dieser Arbeit habe ich gebrauch von Zellen aus einem Cre-induzierbaren $BRAF^{V600E}$ Mausmodell mit gleichzeitiger Deletion von Ink4a/Arf gemacht. Die folgenden Daten zeigen, dass die Expression von $BRAF^{V600E}$ zu einer Erhöhung der symmetrischen Zellteilung in NSC, einer Erhöhung der proliferativen Kapazität, und einer Abnahme des Differenzierungspotentials führt. Außerdem zeige ich, dass die spezifische Inhibierung von $BRAF^{V600E}$ mit dem FDA zugelassenen Medikament vemurafenib (PLX4032/PLX4720) sowohl zu einer Wiederherstellung des Differenzierungspotenzials als auch eine Verringerung der Proliferation und selbst erneuernder NSCs führt.

Table of contents

1 Introduction

1.1 Neural stem cells and neural development

Stem cells are defined as pluripotent or multipotent cells and characterised by their capacity to self-renew and their ability to generate progeny that can differentiate into various other cell types. While pluripotent cells can differentiate into any of the three primary germ layers (endoderm, ectoderm and mesoderm) and thus any cell type in the adult body, multipotent cells can only give rise to a very limited number of cell types (Gage, 2000; Weissman, 2000). Although stem cells are more commonly found during embryonic development, they also are found throughout the adult body where they (endothelial, hematopoietic, mesenchymal and neural stem cells) serve the purpose of tissue renewal and homeostasis (Seaberg and van der Kooy, 2003; Watt and Hogan, 2000).

Neurogenesis continues throughout adult life in adult mammalian brains neural stem cells (NSCs) can be found most commonly in the subventricular zone (SVZ), the wall lining the lateral ventricle, and the hippocampus (Cameron and Gould, 1996; Lois and Alvarez-Buylla, 1994). NSCs residing in the SVZ are relatively quiescent and give rise to actively proliferating progenitor cells (also known as transit amplifying cells, TAPs) (Doetsch et al., 1999). These TAPs have been found to generate fate-restricted intermediary progenitors such as neural or glial restricted progenitors, also referred to as neuroblasts and glioblasts, which respectively give rise to either neurons, or oligodendrocytes and astrocytes (Figure 1-1).

NSCs isolated from the SVZ can be cultured as neurospheres under presence of EGF and non-adhesive surfaces (Reynolds and Weiss, 1992), and have been shown to generate neurons, astrocytes and oligodendrocytes *in vitro* (Weiss et al., 1996). Along the oligodendrocyte lineage arm glioblasts are found as tripotential glial-restricted progenitors (GRPs), which gives rise to Type-1 astrocytes and bipotential oligodendrocyte-type-2 astrocyte progenitors (O2-A/OPCs) (Gregori et al., 2002). OPCs can then differentiate into astrocytes and oligodendrocytes (Figure 1-1). These cell stages can be identified throughout differentiation using specific marker combinations.

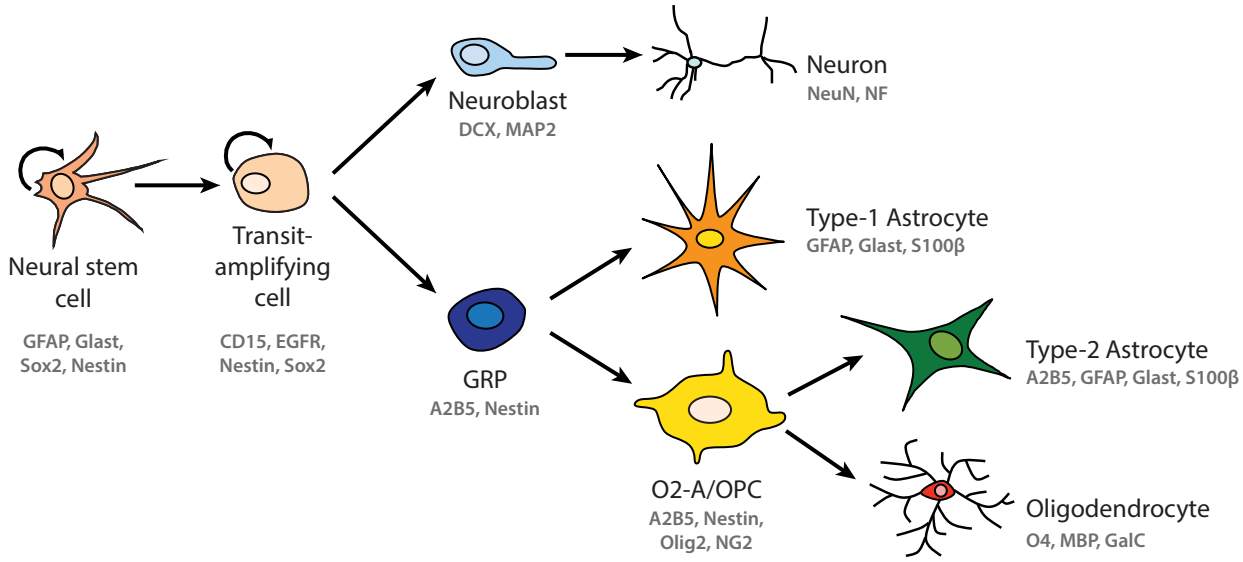

Figure 1-1: Lineage progression of neural stem cells to neurons, astrocytes and oligodendrocytes and associated markers.
A Overview of neural lineages, divided into neurons, arising solely from neuroblasts; astrocytes and oligodendrocytes, both produced from similar precursors. Transit amplifying cells (TAPs) can further give rise to glial restricted progenitors (GRP), which produce oligodendrocyte-type-2 astrocyte progenitors/oligodendrocyte progenitor cells (O2A/OPC) and Type-1 astrocytes. Type-1 and type-2 astrocytes differ morphologically, and in the absence of A2B5 in the former, but not the latter. Markers for the cell stages are listed below each type.
GFAP = glial fibrillary acidic protein; Glast = glutamate aspartate transporter; EGFR = epidermal growth factor receptor; DCX = doublecortin; MAP2 = microtubule-associated protein 2; NeuN = neuronal nuclear antigen; O4 = Oligodendrocyte antigen; MBP = myelin basic protein; GalC = galactocerebroside

Exact classification of adult NSCs, however, remains tricky; they express Nestin and Sox2, as embryonic radial glial cells, as well as glial fibrillary acidic protein (GFAP) and glutamate aspartate transporter (Glast), both also found expressed in astrocytes. A subpopulation of GFAP-expressing SVZ NSCs has also been found enriched for CD15 (also known as SSEA-1 or Lewis X), an extracellular carbohydrate that can be used to identify murine pluripotent stem cells (Capela and Temple, 2002). While $CD15^+$ populations can be divided into subpopulations expressing and absent of the classical stem cell marker CD133, $CD15^+$ cells importantly can form neurospheres, self-renew and differentiate *in vitro*, and $CD15^+$ cells isolated from $CD15^+/CD133^-$ neurospheres have been found capable of forming intracranial tumours in mice (Mao et al., 2009; Son et al., 2009). Furthermore, cells isolated from mouse embryonic cortex and enriched for CD15 have been shown to give rise to two cell types, one with high and one with low activity of epidermal growth factor receptor (EGFR), corresponded with TAPs and GRPs respectively (Sun et al., 2005).

Both oligodendrocyte lineage progenitors are marked by expression of Nestin and cell surface A2B5 antigens, whereas GRP give rise to $A2B5^-$ type-1 astrocytes, and OPCs give rise to $A2B5^+$ type-2 astrocytes, both of which are also $GFAP^+/Glast^+/S100\beta^+$.

In addition, OPCs also express the proteoglycan NG2 and Olig2, a basic helix-loop-helix transcription factor essential during OPC development, and also give rise to oligodendrocytes marked by expression of galactocerebrocide (GalC), myelination agents (e.g. myelin basic protein, MBP) and oligodendrocyte marker O4. In turn, neuronal progenitors can be identified by expression of the neuronal migration protein doublecortin (DCX) and microtubule-associated protein 2 (Map2). Terminally differentiated neurons express the nuclear neuronal marker NeuN and neuron specific intermediary filaments, neurofilaments (NF).

During neurogenesis, which also occurs in adults in the SVZ, this lineage progression is achieved primarily by asymmetric cell division, where following mitosis the two daughter cells have different fates. Defects in the underlying asymmetric cell division machinery could lead to a reduction in neurogenesis, excess in proliferating cells and, ultimately, cancer.

1.2 Asymmetric cell division and its role in development and cancer

As an organism grows from a single fertilised oocyte, stem cells need to expand and differentiate. They achieve this either through direct transformation, symmetric or asymmetric division. Symmetric cell division is the mechanism behind clonal expansion, while asymmetric cell division (ACD) can simultaneously maintain the stem cell population and give rise to a committed daughter (Figure 1-2).

At the heart of the ACD mechanism lies the *par* (partitioning defect) complex, consisting of Par-3, Par-6 and atypical protein kinase C (aPKC), which was initially investigated in *C. elegans* and *D. melanogaster* and has been found conserved in vertebrates (Etemad-Moghadam et al., 1995; Hung and Kemphues, 1999; Kemphues et al., 1988; Rolls et al., 2003). It links astral microtubules to the apical plasma membrane using adaptor proteins (such as Discs large, Dlg) and thus provides an apical-basal orientation for the mitotic spindle (Knoblich, 2010; Schaefer et al., 2001; Siller et al., 2006). Basal localisation of the cell fate determinants Prospero and Numb is also required for correct asymmetric cell division. Prospero is a transcription factor that regulates glial identity and is localised to the basal membrane by binding to the adapter protein Miranda (Choksi et al., 2006). Numb inhibits Notch signalling, which is widely involved in cell fate regulation during development, and is anchored to the basal plasma

membrane by partner of numb (Pon) (Berdnik et al., 2002; Lu et al., 1999; Rhyu et al., 1994) (Figure 1-3).

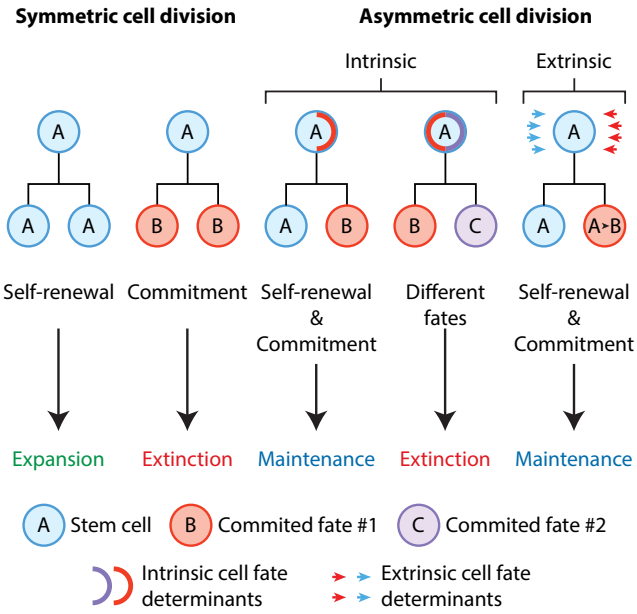

Figure 1-2: Two principal modes of dividing: symmetric and asymmetric cell division.
Symmetric cell division leads to daughter cells of equal fate; either leading to clonal expansion, or maturation and often extinction of the cell line. Asymmetric cell division (ACD) always leads to daughters of divergent fate; either two different committed daughters, or one stem cell and one committed cell. Furthermore, ACD can be initiated through localisation of intrinsic cell fate determinants, such as protein complexes or mRNA, or through extrinsic cell fate determinants such as chemokines or morphogen gradients. Expansion, extinction and maintenance refers to the stem cells (adapted from Tajbakhsh et al., 2009).

The cytoskeletal protein lethal giant larvae (Lgl) has been shown to regulate *par* complex dependant phosphorylation of Miranda, Numb, and Pon, thereby further regulating basal localisation of these factors (Atwood and Prehoda, 2009; Wirtz-Peitz et al., 2008). Currently, the mechanisms of ACD have been well characterised in *D. melanogaster*, mutations in *lgl* and *dlg* have been found to cause tumours in *D. melanogaster* (Lee et al., 2006), but the exact role and function of these proteins in asymmetric cell division in mammalian stem cells remains an issue of on-going research.

While there is evidence for ACD in stem cells of skin, muscle, gut, mammary glands, the hematopoietic system and brain, it remains best understood in neural progenitor cells. Par proteins accumulate at the apical membrane, but minor interferences can cause oblique cleavages (divisions neither perpendicular, nor horizontal to the apical-basal polarity) and in that process lead to an asymmetric distribution of Par3 in the progeny. Following, the levels of cell fate determinant Notch are increased in the high-Par3 daughter, which remains a stem cell, whereas the

daughter cell inheriting low Par3 also has low levels of Notch, and goes on to differentiate (Bultje et al., 2009).

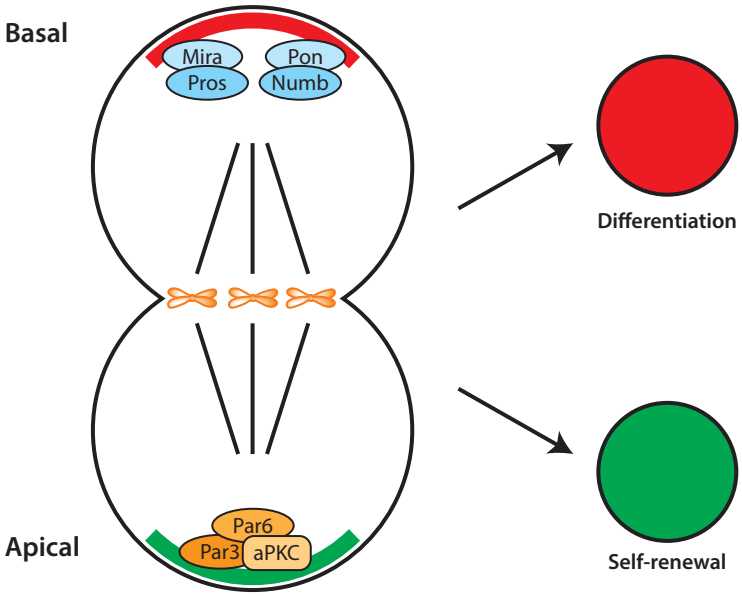

Figure 1-3 Localisation of cell fate determinants during asymmetric cell division.
Localisation of the par complex, consisting of Par3, Par6 and atypical protein kinase C (aPKC), defines the apical end during asymmetric cell division. aPKC by itself, has been shown to phosphorylate Miranda (Mira), which then leads to its basal localisation with Prospero (Pros). Lgl acts as an antagonist in this process. Furthermore, aPKC and Par6 bind Lgl in early metaphase, which is later replaced by Par3. The complete par complex then phosphorylates Numb, which then localises to the basal end with its adapter protein partner of numb (Pon). Apical, aPKC containing daughter cells go on to self-renew, while the basal daughter cell undergoes differentiation most notably by Numb-mediated Notch signalling.

Recent research has shown, that EGFR segregates asymmetrically and plays a role in neural stem cell fate determination (Sun et al., 2005). Further, constitutive signalling of EGFR has been found to inhibit differentiation of oligodendrocyte progenitors (Ivkovic et al., 2008). In summary, disruption of ACD leads to less differentiation and an increase in self-renewal, a hallmark of cancer.

Results from our lab further indicate, that decreased asymmetric divisions in oligodendrocyte progenitors are signs of glioma precursors (Sugiarto et al., 2011). Furthermore, previous research shows that mouse and human oligodendrogliomas, gliomas thought to have oligodendrocyte origin, share more markers with OPCs than NSCs, supporting the hypothesis of OPCs as origin of gliomas (Persson et al., 2010).

1.3 Gliomas, how they arise and theories on their origin

Cancer is a common cause of death across the world and is found in people of all ages. Brain tumours in particular make up only 1% of all cancers, but patients have an overall poor survival (Howlader et al., 2013; Siegel et al., 2013). Brain tumours are

graded by the world health organisation (WHO) depending on malignancy, growth speed and morphology in low-grade (grade I and II) and high-grade (grade III and IV) tumours. They are further classified by their morphology as astrocytoma, glioblastoma, oligodendroglioma, mixed glioma, ependymoma, malignant glioma, and a few rare histological variations (Louis et al., 2007). Oligodendrogliomas and ependymomas occur rarely (~10-20% of all brain tumours), and are only found in grades I-III (Dolecek et al., 2012; Louis et al., 2007). Astrocytomas, in contrast, represent the most common form of brain tumours, are found in all grades and more than half of all cases are the particularly aggressive glioblastoma multiforme (GBM, grade III-IV) (Dolecek et al., 2012). Astrocytomas have a total age-adjusted incidence of 6.6 per 100.000, with pilocytic astrocytomas leading in prevalence of under-35-year-olds and GBM accounting for more than half of all cases in patients aged 35 and up. Additionally, glioblastoma multiforme is the most aggressive form, with a 5-year survival rate of less than 5% (Dolecek et al., 2012).

Gliomas are currently classified by morphology, but in recent efforts from the Cancer Genome Atlas (TCGA) consortium they classified gliomas into four distinct subtypes, depending on their genetic profile: neural, proneural, classic and mesenchymal (Verhaak et al., 2010). However, it still remains hotly debated cell types are the origin.

In support of NSCs as glioma origin, GFAP or Nestin driven deletion of *p53* in mouse brains reflected human glioma pathologies (Wang et al., 2009). Furthermore, deletion of the tumour suppressors $p16^{Ink4a}$ and $p19^{Arf}$ (both encoded by the *CDKN2A* locus) combined with EGFR overexpression in cultured neurospheres provided the capacity to induce gliomas after intracranial injection into immunocompromised mice, reconfirming the NSC-origin model (Bachoo et al., 2002; Ligon et al., 2007).

However, two possibilities remain: the defective NSCs or progenitors derived from these NSCs are the cell-of-origin for gliomas.

A transgenic mouse model with S100β-driven activation of the *v-erbB* oncogene, a protein structurally similar to EGFR with a ligand-independent constitutive tyrosine kinase activity, illustrated that mature cells could contribute to glioma formation (Persson et al., 2010; Weiss et al., 2003). While S100β is often used as mature astrocyte marker, it is activated as $GFAP^{+}$ cells lose their capability to form neurospheres (Hachem et al., 2005; Raponi et al., 2007).

EGFR is a receptor tyrosine kinase (RTK), which signals BRaf, a member of the Ras/Raf/MEK/ERK protein kinase (also known as mitogen-activated protein kinase, MAPK) pathway. BRaf has been found activated, mutated or as oncogenic fusion gene in a 4% of GBM. The activating mutation $BRaf^{V600E}$ is often found in grade II-IV tumours and is highly associated with young patient age (Schiffman et al., 2010; Schindler et al., 2011). It's role in tumour development, however, remains an issue of on-going research.

1.4 The MAPK Pathway and its role in cancer

The canonical MAPK pathway is triggered by a wide variety of cues, most notably cell stress, growth factors, cytokines and mitogens, often mediated through RTKs such as EGFR (Figure 1-4). The MAPK pathway is known to regulate proliferation, differentiation and apoptosis (Blalock et al., 1999; Chang et al., 2003) and the involved proteins are commonly found mutated in cancer.

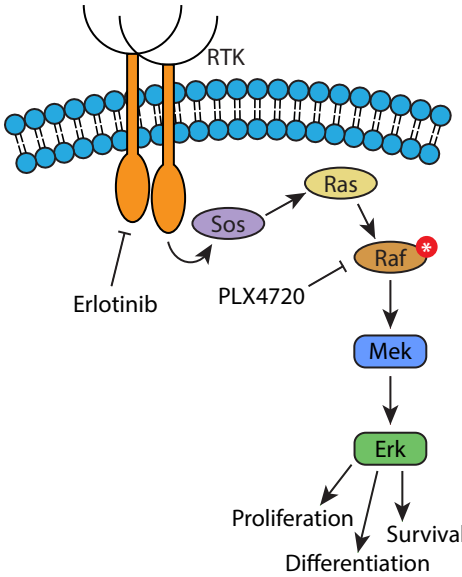

Figure 1-4 Schematic overview of the MAPK Pathway.
Upon binding of the ligand, the receptor tyrosine kinase (RTK) dimerises and can then activate the guanidine exchange factor Sos. Activated Sos then can drive removal of GDP from a Ras superfamily protein, which can then bind GTP and phosphorylate Raf.
Raf can now phosphorylate Mek, which can then phosphorylate the mitogen activated protein kinase MAPK or Erk. This final kinase goes on to activate several transcription factors regulating proliferation, differentiation and apoptosis.
Drugs used to inhibit the MAPK pathway in this thesis are PLX4720 (vemurafenib), which can specifically inhibit $BRaf^{V600E}$ (indicated by a red circle), and Erlotinib, an inhibitor of EGFR phosphorylation.

The Ras family of proteins encompasses three variants, HRAS, KRAS and NRAS, which have a highly conserved N-terminal GTPase region and are known oncogenes. They are bound to the membrane, when activated exchange GDP for GTP and have been found to activate both the PI3K and Raf to varying degrees (Peyssonnaux et al., 2000).

Similarly, the Raf protein family also has three members: A-Raf, B-Raf (in following referred to as BRaf), and c-Raf (also referred to as Raf-1). They have three distinct domains, an N-terminal Ras binding domain (CR1), a regulatory domain (CR2) and the catalytic kinase domain (CR3), and their activity varies across tissues (Pritchard et al., 1996; Van Aelst et al., 1993). BRaf, most importantly, is highly expressed in neural tissue (Barnier et al., 1995). Moreover, deletion of BRaf in neuronal

precursors showed decreased myelination illustrating its importance in neuronal differentiation and oligodendrocyte maturation (Galabova-Kovacs et al., 2008).

Aberrations in BRaf involve either a constitutively active kinase domain, increases in copy number, gene amplification, or a combination of the above. The kinase domain is found constitutively activated either through a recently discovered fusion with KIAA1549, a gene of unknown function, or by mutation in the kinase domain (Davies et al., 2002; Jones et al., 2008). The $BRaf^{V600E}$ variant is the most common, accounting for 80% of the mutations, and is found most frequently in melanoma (50%), papillary thyroid carcinoma (30%), ovary carcinoma (20%) and colorectal cancer (15%), while in contrast it is found in 4% of gliomas with increased prevalence in children (Schiffman et al., 2010; Schindler et al., 2011; Zebisch and Troppmair, 2006).

Hyper-activation of the MAPK pathway has been demonstrated to lead to senescence, signalled through $p16^{Ink4a}$ and $p19^{Arf}$ (Ink4a/Arf, encoded by the CDKN2A locus) (Jacob et al., 2011). Furthermore, activation of BRaf in NSCs by transduction with $BRaf^{V600E}$ cDNA has been shown to lead to transformation at first, and then $p16^{Ink4a}$-regulated senescence (Raabe et al., 2011). Deletion of CDKN2A has been reported in gliomas and found associated with $BRaf^{V600E}$ in 70% of higher-grade tumours, which recently led to the paediatric malignant astrocytoma mouse model through the combination of $BRaf^{V600E}$ and $Ink4a/Arf^{-/-}$ (Horbinski et al., 2010; Rodriguez et al., 2011; Schiffman et al., 2010).

The work presented here makes use of a genetically modified mouse model with Cre recombinase-inducible $BRaf^{V600E}$ expression and concomitant Ink4a/Arf deletion to address questions posed on the cell-of-origin of gliomas and the influence of $BRaf^{V600E}$ on the ACD machinery (Dankort et al., 2007).

1.5 The $BRaf^{V600E}$ model system

Studying the effect a mutant gene has in vitro is relatively simple and can be achieved by introducing the mutation with a plasmid or viral vector. This, however, is a highly artificial system, and especially when studying diseases such as cancer it is desirable to employ an organism-scale model often ideally including an inducible mutation.

$BRaf^{V600E}$ (initially identified as V599E) was first discovered in melanoma and has since seen several efforts for small molecule-based inhibition (Davies et al., 2002).

Vemurafenib (also known as PLX4032, or the tool compound PLX4720) is the first drug to specifically inhibit $BRaf^{V600E}$, has been FDA-approved for late stage melanoma is currently in early stages of several clinical trials for melanoma as well as entering clinical trials for treatment of paediatric astrocytomas (Bollag et al., 2010; Chapman et al., 2011; Sala et al., 2008). Mechanistically vemurafenib selectively binds to the ATP binding pocket of $BRaf^{V600E}$, but not wild-type BRaf ($BRaf^{WT}$) (Tsai et al., 2008), however it has also been shown to activate the MAPK pathway in $BRaf^{WT}$ melanoma cell lines (Halaban et al., 2010; Hatzivassiliou et al., 2010).

To date, tumorigenic BRaf activation has only been studied in tumour-derived cell lines, which do not allow isolating the effect of $BRaf^{V600E}$ specifically and it's blockage. Several human glioblastoma cell lines have been used to study $BRaf^{V600E}$, however they are genetically heterogeneous and found either heterozygous or homozygous for mutant BRaf (Nicolaides et al., 2011).

The genetically engineered mouse model (GEMM) obtained by our lab expresses a Cre recombinase-inducible $BRaf^{V600E}$ mutation (*$BRaf^{CA}$*, Figure 1-5) and LoxP flanked exons 2 and 3 of the *CDKN2A* locus ensuring deletion of both tumour suppressors $p16^{Ink4a}$ and $p19^{Arf}$ (Ink4a/Arf), both easily confirmable by PCR (Aguirre et al., 2003; Dankort et al., 2007). Deletion of Ink4/Arf, in addition to being highly correlated with $BRaf^{V600E}$ in high-grade tumours, serves as a background mutation as $BRaf^{V600E}$ on its own has been shown to induce senescence (Raabe et al., 2011).

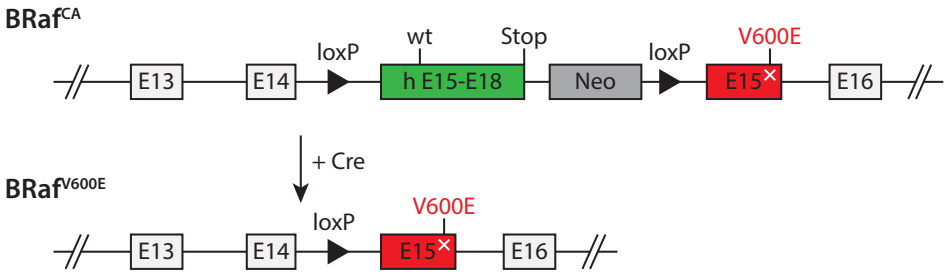

Figure 1-5: Schematic representation of the $BRaf^{CA}$ genotype and the generation of $BRaf^{V600E}$ through induction with Cre recombinase.
$BRaf^{CA}$ was created by introducing the human cDNA for exons 15-18 (h E15-E18) into the intron between mouse exon 14 and 15. This produces normal BRaf, upon Cre-mediated recombination the human cDNA is deleted and the $BRaf^{V600E}$ mutant is produced (adapted from (Dankort et al., 2007)).

Furthermore, our employed GEMM allows localised induction of $BRaf^{V600E}$ by *intracranial* delivery of adenovirus expressing Cre recombinase and subsequently allows the histopathological study of its effects in brain tumours *in vivo*. Research in our lab has shown, that we can induce brain tumours, which are morphologically similar to

GBM (Figure 1-6A and B) and express similar markers (data not shown). Moreover, we showed that mice with tumours driven by ubiquitous Cre expression died just as soon as tumours from transformed SVZ NSCs, which suggests a common cell of origin (Figure 1-6C).

In addition to *in vivo* studies, this model provides interesting possibilities for in vitro studies too: by isolating NSCs harbouring $BRaf^{CA}$ and inducing $BRaf^{V600E}$ *in vitro* and its effects on various cellular mechanisms underlying tumorigenesis, such as asymmetric cell division and differentiation.

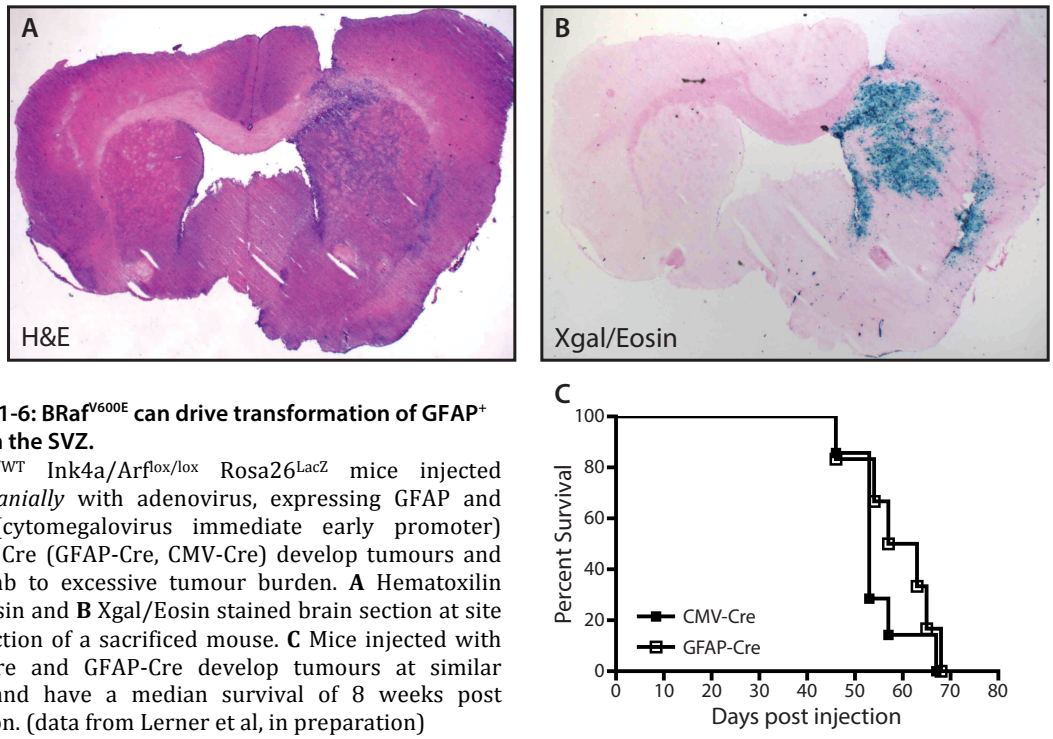

Figure 1-6: $BRaf^{V600E}$ can drive transformation of $GFAP^{+}$ NSCs in the SVZ.
$BRaf^{CA/WT}$ $Ink4a/Arf^{lox/lox}$ $Rosa26^{LacZ}$ mice injected *intracranially* with adenovirus, expressing GFAP and CMV (cytomegalovirus immediate early promoter) driven Cre (GFAP-Cre, CMV-Cre) develop tumours and succumb to excessive tumour burden. **A** Hematoxilin and eosin and **B** Xgal/Eosin stained brain section at site of injection of a sacrificed mouse. **C** Mice injected with CMV-Cre and GFAP-Cre develop tumours at similar rates and have a median survival of 8 weeks post injection. (data from Lerner et al, in preparation)

2 Aims of this project

Mutations in Raf family proteins and their upstream activators Ras and EGFR are associated with many forms of cancers, and BRaf in particular has been found mutated as $BRaf^{V600E}$ in paediatric astrocytomas. However, it is unclear which function $BRaf^{V600E}$ has in regards to tumour initiation, origin and maintenance.

This thesis aims to answer some of these questions and in specific addresses the following:

Aim 1: Establish an isogenic $BRaf^{V600E}$ culture model. Using mice expressing $BRaf^{CA}$ I will isolate healthy cells from the subventricular zone. This will allow me to study how BRaf activation changes cells *in vitro* and leads to tumour initiation.

Aim 2: Understand the impact of BRaf activation on neural stem and progenitor cell proliferation. Using isogenic cell lines and tumour cell lines I will test proliferation following $BRaf^{V600E}$ induction and its inhibition. Doing so will tell us if activation of BRaf confers proliferative advantages and if cells benefit from more than one copy and could infer more effective treatment regiments.

Aim 3: Unravel the influence BRaf activation has on neural lineage differentiation. Using the established culture model I will investigate the changes of $BRaf^{V600E}$ expression and its inhibition on generation of neurons, oligodendrocytes and astrocytes. This will help us understand if activation of BRaf leads to transformation of either neural stem cells or progenitor cells and if this process can be reversed by chemical blockage of $BRaf^{V600E}$.

Aim 4: Elucidate how oncogenic $BRaf^{V600E}$ alters asymmetric cell division of neural stem and progenitor cells. Using isogenic *in vitro* modified cell lines I will analyse how expression of $BRaf^{V600E}$ and inhibition thereof affect neural stem and progenitor cells' ability to self-renew and generate daughters of different fate. Results gained here will give insight on which cells $BRaf^{V600E}$-driven tumours arise from and if specific inhibition of $BRaf^{V600E}$ can slow this process.

3 Methods

3.1 Culturing mouse neurospheres

Subventricular zone (SVZ)-NSCs were isolated and grown from adult mice as previously described (Silber et al., 2008) with minor modifications. Dissected SVZ tissue from 2-month old mice was dissociated using papain (Worthington). Cells were grown in Neurobasal-A media (Invitrogen) supplemented with 20 ng/mL epidermal growth factor (EGF, Sigma), 20 ng/mL basic fibroblast growth factor (bFGF, Peprotech), 1x B27 supplement without Vitamin A (Invitrogen), 100 units/mL penicillin, 100 µg/mL streptomycin and 292 µg/mL L-glutamine on low adherent plates. Cultures were maintained at 37°C and 5% CO_2. Cells were passaged by incubating in Accumax (Innovative Cell Technologies) for 5 minutes and triturated during resuspension. Media was changed every 2.5 days.

3.2 Induction of tumours *in vivo*

Two-month old mice received intracranial injections into the SVZ with adenovirus expressing Cre recombinase under the CMV promoter. Upon exhibiting behavioural signs of tumour burden they were sacrificed, tumour tissue was isolated and dissociated with papain. Tumour cells were cultured identically to unmodified, transgenic neurospheres.

3.3 Generation of mutant cell lines

Before transduction neurospheres are dissociated using Accumax for 5 minutes and triturated gently. Cells are counted to calculate the volume of virus required.

$$\text{Virus}[\mu\text{L}] = \frac{\text{number of cells seeded}}{\text{virus titer } [IFU/mL]} \times MOI$$

The virus titer was determined during virus production and purification and the MOI reflects the ratio of virus particles per cell, here selected as 50. An adenovirus expressing a Cre-GFP fusion protein is added in a control well to determine if the virus amount is sufficient. Once ensured the adenovirus with CMV driven Cre expression is added and cells are incubated at 37°C over night and medium is replaced the following day. Transformation and deletion was confirmed by genotyping.

3.4 Genotyping of cells and tissue

Both tissue and cells can be genotyped with the same protocol. The sample is incubated with STE buffer (0.1M NaCl, 10mM Tris pH8, 1mM EDTA) and 20 µg/mL proteinkinase K (Qiagen) at 55°C for 2 hours to over night. Before PCR proteinkinase K is inactivated by incubating at 95°C for 10 minutes. Primer pairs BRaf-fw (5'-tgagtatttttgtggcaactgc-3') and BRaf-rev (5'-ctctgctgggaaagcggc-3'), are used to differentiate between $BRaf^{WT}$ (185 bp), $BRaf^{CA}$ (308 bp) and $BRaf^{V600E}$ (335 bp) (Dankort et al., 2007). Deletion of Ink4a/Arf was confirmed using the primer pairs Ink-fw (5'- ccaagtgtgcaaacccaggc-3') and Ink-rev (5'-ttgttggcccaggatgcc-3'), allowing the distinction between $Ink4a/Arf^{WT}$, $Ink4a/Arf^{lox}$ and $Ink4a/Arf^{-}$ as previously described (Aguirre et al., 2003).

3.5 Proliferation assay

Cells were dissociated and plated on black, optical bottom 96-wells (Nunc), previously coated with 10 µg/mL laminin (Sigma) at 37°C for at least 3 hours, at a concentration of 2000 cells/well (500 cells/well for tumour tissue). Measuring is done by adding 10 µL of 10x alamarBlue (Invitrogen) to the wells, incubating for 1 hour at 37°C, and reading the fluorescence at 610nm (excitation at 540nm) using a plate reader. Then, drug can be added to wells for inhibition experiments and measurements can continue the following days. Measurements were taken in triplicates. Wells used for measurements need to be discarded.

3.6 Differentiation assay

Cells are dissociated and plated in Lab-Tek II CC2 chamber slides (Nunc), previously coated with 10 µg/mL laminin (Sigma) for at least 3 hours, at a concentration of 15000 cells/chamber. After two days of growth and attachment media is exchanged for differentiation promoting media, which is then carefully replenished every two days. Growth media was supplemented with 2 % fetal calf serum (UCSF cell culture facility), or 60 nM triiodothyronine (T3; Sigma) and 100 ng/mL insulin-like growth factor 1 (IGF-1; Sigma) instead of EGF and FGF for undirected and oligodendrocyte directed growth respectively. The cells were fixed with 4 % paraformaldehyde (PFA; Electron Microscopy Sciences) at room temperature for 10 minutes, washed and stored in PBS (UCSF cell culture facility) with 0.1 % sodium azide (Fisher) or immediately labelled by

immunocytochemistry. Cells grown with inhibitors received drugs upon initial plating in chamber slides.

3.7 Cell pair assay

The cell pair assay is based on a previously described method (Shen et al., 2002) with minor modifications. After dissociation the cells are plated on Terasaki microwell plates (Nunc) at 100 cells and 10 µL per well. After 2 hours of incubation the cells are checked for adherence and even distribution, and then further incubated for a total of 16-24 hours, or one division. Finally, the plate was removed, the cells were fixed with 4 % PFA at room temperature for 10 minutes, washed and stored in PBS with 0.1 % sodium azide (Fisher) or immediately further processed for immunofluorescent labelling. For inhibition experiments drug was added to cells prior to plating.

3.8 Immunocytochemistry

After fixation and washing cells were blocked in blocking buffer (PBS, 0.1 % Triton X-100, 5 % NGS) for one hour, and incubated with the primary antibody in blocking buffer for one hour at room temperature, or over night at 4°C. Appropriate IgGs were used instead of primary antibodies for negative controls. After 3 wash steps with PBS the according secondary antibody was added and incubated in the dark at room temperature for 1 hour. Following one final washing, DNA was stained using DAPI in PBS at room temperature for 5 minutes. Cover slips were fixed to the chamber slides with mounting media, while Terasaki plates could be imaged when kept in PBS.

3.9 Analysis of immunocytochemistry images

Quantitative comparison of immunocytochemically labelled markers is traditionally done by manually recording each occurrence. This method works well for nuclear and, in the case of sparse cell spacing, cytoplasmic markers. However, after several days of growth precise attribution of cytoplasmic labels to their corresponding nuclei in densely packed populations is arguably not possible. Increasing numbers of slides and images per cell line and staining only exacerbates this problem. This challenge was tackled using a software-based method. ImageJ, a freeware image-processing tool, offers a built-in function to measure the average intensity across the entire image. For differentiation assays, it was ensured that all images of each well were taken with identical microscope settings and combined to one slide in ImageJ. After

measuring maximum and minimum cell sizes nuclear markers could be counted using an automated built-in function. For cytoplasmic markers the average intensity across the combined image was measured and divided by the number of cells resulting in a value termed *relative intensity*. During planning stages of this method the resulting relative intensity was compared to manually counted percentages and found to be comparable.

4 Results

4.1 BRaf^{V600E} increases proliferative capacity in adult neural stem cells and tumour-derived cells.

BRafV600E has been identified as a tumour causing mutation in murine models of glioma. To date, the cellular effects of BRaf activation and inhibition in neural stem and progenitor cells, thought to be a potential origin of glioma, have not been studied. Initially, I was interested, if the dosage of BRaf^{V600E}-expression altered proliferative behaviour. To determine this difference two-month-old BRaf$^{WT/WT}$, BRaf$^{WT/CA}$ and BRaf$^{CA/CA}$, all also Ink4a/Arf$^{lox/lox}$, adult mice were sacrificed and NSCs were isolated from the SVZ. The neurospheres were treated with an adenovirus expressing Cre recombinase ubiquitously driven by the CMV promoter (Ad:Ubi-Cre), to induce expression of BRaf^{V600E}. Using an adapted cytotoxicity assay allowed the determination of viable cells every 2 days.

After 5 days of growth the expression of one copy of BRaf^{V600E} showed an increase of proliferative capacity over BRaf^{WT} in adult neural stem cells after 5 days, while a second copy of the V600E mutant did not result in any further growth advantage (Figure 4-1). Longer growth led to confluence and consequently rapid metabolism of AlamarBlue, resulting in an oversaturated readout.

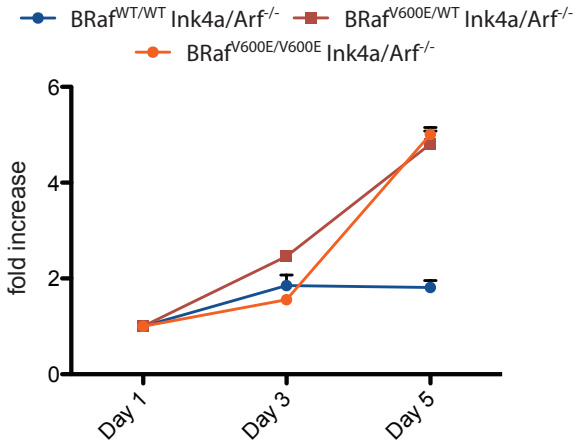

Figure 4-1: BRaf^{V600E} increases proliferative capacity of *in vitro* modified cells.
One copy of BRaf^{V600E} (red) shows an increase of proliferative capacity over BRaf$^{WT/WT}$ (blue), raising the fold-increase from under 2-fold to an increase of more than 4-fold, while a second copy of BRaf^{V600E} (orange) gives no further proliferative advantage after 5 days of growth. Proliferative capacity was determined using AlamarBlue, which upon uptake and metabolic reduction by viable cells produces bright red fluorescence. Absolute values gained from the plate reader were normalised to day one. Where visible black error bars indicate the standard error of the mean (SEM).

Interested if this dosage-independence was an artificial effect, I analysed proliferation of mouse-derived tumour cells from adult BRaf$^{CA/WT}$ Ink4a/Arf$^{lox/lox}$ and BRaf$^{CA/CA}$ Ink4a/Arf$^{lox/lox}$ mice treated with an intracranial injection of either Ad:Ubi-Cre or Ad:GFAP-Cre virus, the latter specifically targeting stem cells in the SVZ, using the same protocol as above. The cells obtained from GFAP-driven BRaf$^{V600E/WT}$ tumours were isolated from exophytic tumour tissue and also grew slowest (Figure 4-2). While BRaf$^{V600E/WT}$ Ink4a/Arf$^{-/-}$ and BRaf$^{V600E/V600E}$ Ink4a/Arf$^{-/-}$ showed little difference in growth speed between CMV- and GFAP-driven viral infections, tumour cells had a proliferative advantage conferred by dosage-dependent BRaf^{V600E}-expression (Figure 4-2).

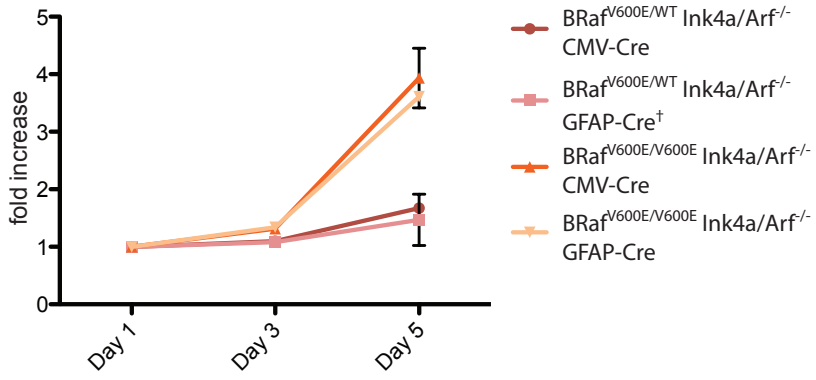

Figure 4-2: BRaf^{V600E} has dosage dependant effect on proliferation in mouse-derived glioma cells.
CMV- and GFAP-driven BRaf$^{V600E/WT}$ Ink4a/Arf$^{-/-}$ (red, and pale red; n=1 and n=2 respectively), as well as CMV- and GFAP-driven BRaf$^{V600E/V600E}$ Ink4a/Arf$^{-/-}$ tumours (orange and pale orange; n=3 and n=1 respectively) show little difference in growth between CMV- or GFAP-driven viral infections. However, tumour cells expressing only one copy of BRaf^{V600E} grew only 2-fold, while cells with two copies grew to more than 4-fold over 5 days.
n=biological replicates, each measured in triplicates

†Cells from GFAP-driven BRaf$^{V600E/WT}$ Ink4a/Arf$^{-/-}$ tumours were isolated from exophytic tissue. Error bars indicate SEM of tumour lines, where applicable.

PLX4720, a tool compound of vemurafenib, has been shown to inhibit growth of malignant glioma cell lines at a concentration of 1µM (Nicolaides et al., 2011). To determine if this inhibition can be recapitulated in *in vitro* modified NSCs the cells were treated with PLX4720 at final concentrations of 1, 10, 20 and 50µM one day after plating and monitored over the course of 6-8 days.

Proliferation assays showed, that BRaf$^{WT/WT}$ Ink4a/Arf$^{-/-}$ cells were not impeded, in fact, their growth was increased with PLX4720 at concentrations of and below 20 µM, when compared against vehicle, consistent with previous reports from human glioma lines (Figure 4-3A) (Nicolaides et al., 2011). One BRaf^{V600E} allele was sufficient to negate this effect and resulted in a decrease of 15% at a drug concentration of 20 µM by day 6

(Figure 4-3B). Cells homozygous for BRaf^{V600E} and Ink4a/Arf deficient showed a 30% decrease at a drug concentration of 5 µM, and up to 50% decrease with 20 µM (Figure 4-3C). PLX4720 dose response proliferation assays on tumour cells were performed at concentrations of 1 and 10 µM showed a similar response.

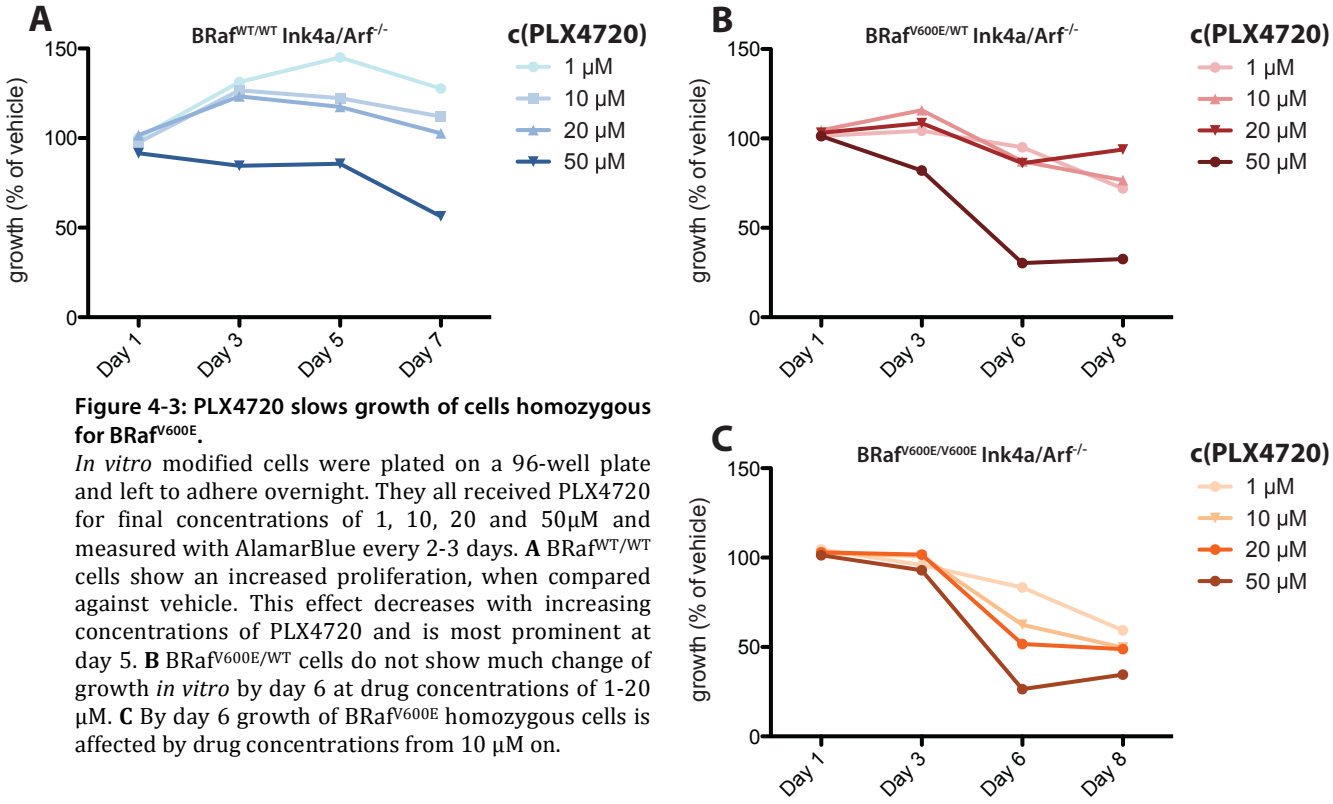

Figure 4-3: PLX4720 slows growth of cells homozygous for BRaf^{V600E}.
In vitro modified cells were plated on a 96-well plate and left to adhere overnight. They all received PLX4720 for final concentrations of 1, 10, 20 and 50µM and measured with AlamarBlue every 2-3 days. **A** BRaf$^{WT/WT}$ cells show an increased proliferation, when compared against vehicle. This effect decreases with increasing concentrations of PLX4720 and is most prominent at day 5. **B** BRaf$^{V600E/WT}$ cells do not show much change of growth *in vitro* by day 6 at drug concentrations of 1-20 µM. **C** By day 6 growth of BRaf^{V600E} homozygous cells is affected by drug concentrations from 10 µM on.

Epidermal growth factor receptor (EGFR) is an upstream activator of BRaf and can be inhibited by Erlotinib, which reversibly binds to the ATP binding site of the receptor. Erlotinib is an FDA-approved drug primarily used in treatment of non-small cell lung cancer (Glover et al., 2004) and has so far shown mixed results in clinical trials treating for glioblastomas (Haas-Kogan et al., 2005; Wick et al., 2011). Drug combination treatment, however can provide additional benefit over single treatment.

To address the idea of combination therapy with PLX4720 an initial dose response proliferation assays for Erlotinib was set up. A drug concentration of 0.5 µM showed an inhibited growth in BRaf$^{WT/WT}$ Ink4a/Arf$^{-/-}$ cells by 70 % after 6 days (Figure 4-4A), in contrast cells with one copy of the V600E-form are only inhibited by 20% after the same duration (Figure 4-4B). Treating *in vitro* modified cells heterozygous and homozygous for BRaf^{V600E} with the combination of 0.5µM Erlotinib and 1µM PLX4720 for 5 days, however, shows an increased inhibition greater than the sum of their parts (Figure 4-4C).

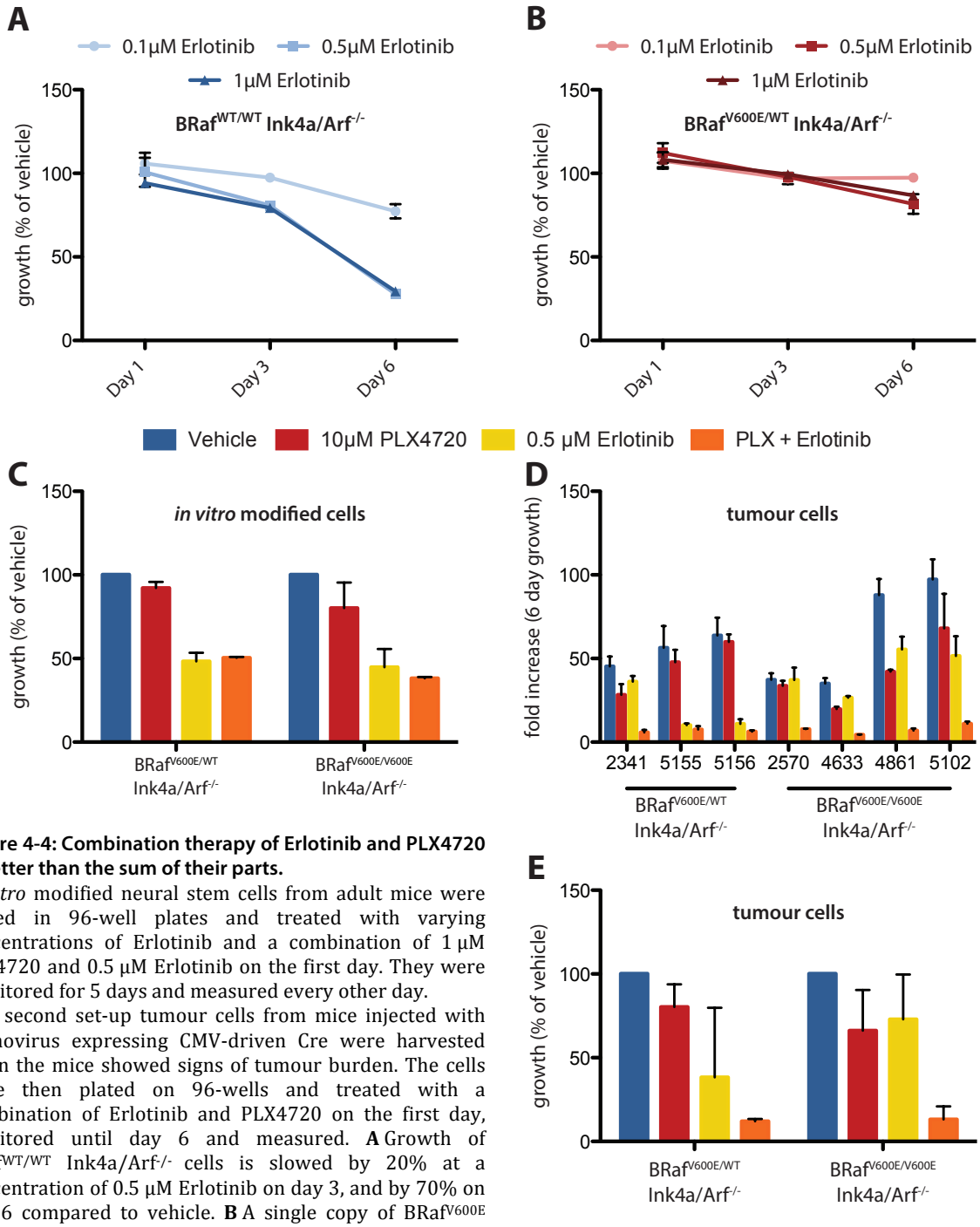

Figure 4-4: Combination therapy of Erlotinib and PLX4720 is better than the sum of their parts.
In vitro modified neural stem cells from adult mice were plated in 96-well plates and treated with varying concentrations of Erlotinib and a combination of 1 μM PLX4720 and 0.5 μM Erlotinib on the first day. They were monitored for 5 days and measured every other day.
In a second set-up tumour cells from mice injected with adenovirus expressing CMV-driven Cre were harvested when the mice showed signs of tumour burden. The cells were then plated on 96-wells and treated with a combination of Erlotinib and PLX4720 on the first day, monitored until day 6 and measured. **A** Growth of $BRaf^{WT/WT}$ $Ink4a/Arf^{-/-}$ cells is slowed by 20% at a concentration of 0.5 μM Erlotinib on day 3, and by 70% on day 6 compared to vehicle. **B** A single copy of $BRaf^{V600E}$ negates Erlotinib mediated EGFR inhibition on day 3, by day 6 proliferation is only reduced by 20% compared to vehicle. **C** Combination treatment of two heterozygous and two homozygous $BRaf^{V600E}$ cell lines for 5 days shows that inhibition of growth can be greatly improved using both 0.5 μM Erlotinib and 1 μM PLX4720. **D** Treating tumour cell lines with a combination of PLX4720 and Erlotinib yields a strong inhibition in both heterozygous and homozygous tumour cell lines. Error bars indicate SEM of replicates. **E** Averaging the tumour cell lines from above and normalising to the vehicle also shows a consistent response to the combination therapy reducing $BRaf^{V600E/WT}$ $Ink4a/Arf^{-/-}$ and $BRaf^{V600E/V600E}$ $Ink4a/Arf^{-/-}$ to 12% and 13% growth over 6 days compared to vehicle. Error bars indicate SEM of average values.

Tumour cells isolated from the SVZ of 3 $BRaf^{CA/WT}$ and 4 $BRaf^{CA/CA}$ adult mice injected with Ad:Ubi-Cre were treated with 0.5 μM Erlotinib and 1 μM PLX4720 for 6 days. PLX4720 and Erlotinib on their own show decreased growth in $BRaf^{V600E/WT}$ and $BRaf^{V600E}$ heterozygous tumour cells when compared against vehicle. Combining both

drugs yielded low, comparable growth rates in all cell lines over 6 days, regardless of their response to single drug treatments (Figure 4-4D). Averages show comparable levels of 90% growth inhibition after 6 days in both heterozygous and homozygous $BRaf^{V600E}$ tumour cell lines compared to vehicle (Figure 4-4E).

4.2 $BRaf^{V600E}$ reduces differentiation potential of adult neural stem cells

Neurogenesis continues in adult mammals, is most prominent in the subventricular zone (SVZ) and has been shown to require asymmetric cell division (Noctor et al., 2004). Deregulation of the ACD-machinery in *D. melanogaster* neuroblasts is known to lead to accumulation of undifferentiated stem and progenitor cells (Caussinus and Gonzalez, 2005).

To investigate if constitutively active $BRaf^{V600E}$ shows an effect on differentiation of neural stem cells, early passages (p4-p8) *in vitro* modified $BRaf^{WT/WT}$ $Ink4a/Arf^{-/-}$ and $BRaf^{V600E/WT}$ $Ink4a/Arf^{-/-}$ cells were grown under undirected differentiation conditions for 7 days and stained for neural lineages and GFAP. Cells expressing $BRaf^{V600E}$ also showed decreased positivity for all markers (Figure 4-5A), as well as a change in morphology, suggesting further astrocyte/glial lineage progression (Figure 4-5B, C). The greater number of DCX and MAP2 double positives in $BRaf^{WT/WT}$ suggests cells progress more along the neuronal lineage without constitutive expression of the V600E form (Figure 4-5D-G).

The oligodendrocyte transcription factor Olig2 and S100-family member S100β are found in nuclei of oligodendrocyte progenitor cells (OPCs), whereas nuclear export of Olig2 has been found to mediate differentiation of glial precursors to astrocytes upon brain-injury (Magnus et al., 2007). To determine if $BRaf^{V600E}$ influences oligodendrocyte differentiation the cells were then again grown under undirected differentiation conditions for 5 days and stained for Olig2, S100β, NeuN, GFAP and Nestin. S100β and Olig2 were found increased under expression of $BRaf^{V600E}$ and only half as many cells as in the wild type expressed NeuN, but saw an increase in both S100β and Olig2 (Figure 4-6A). Furthermore, $BRaf^{V600E}$ expressing cells showed a four-fold increase and exclusive nuclear retention of Olig2 expression and double the amount of $S100\beta^{+}$ cells (Figure 4-6B-E). In contrast, Olig2 was often found in the cytoplasm of $BRaf^{WT/WT}$ cells, a possible indication for an increase in astrocytic differentiation (Setoguchi and Kondo, 2004).

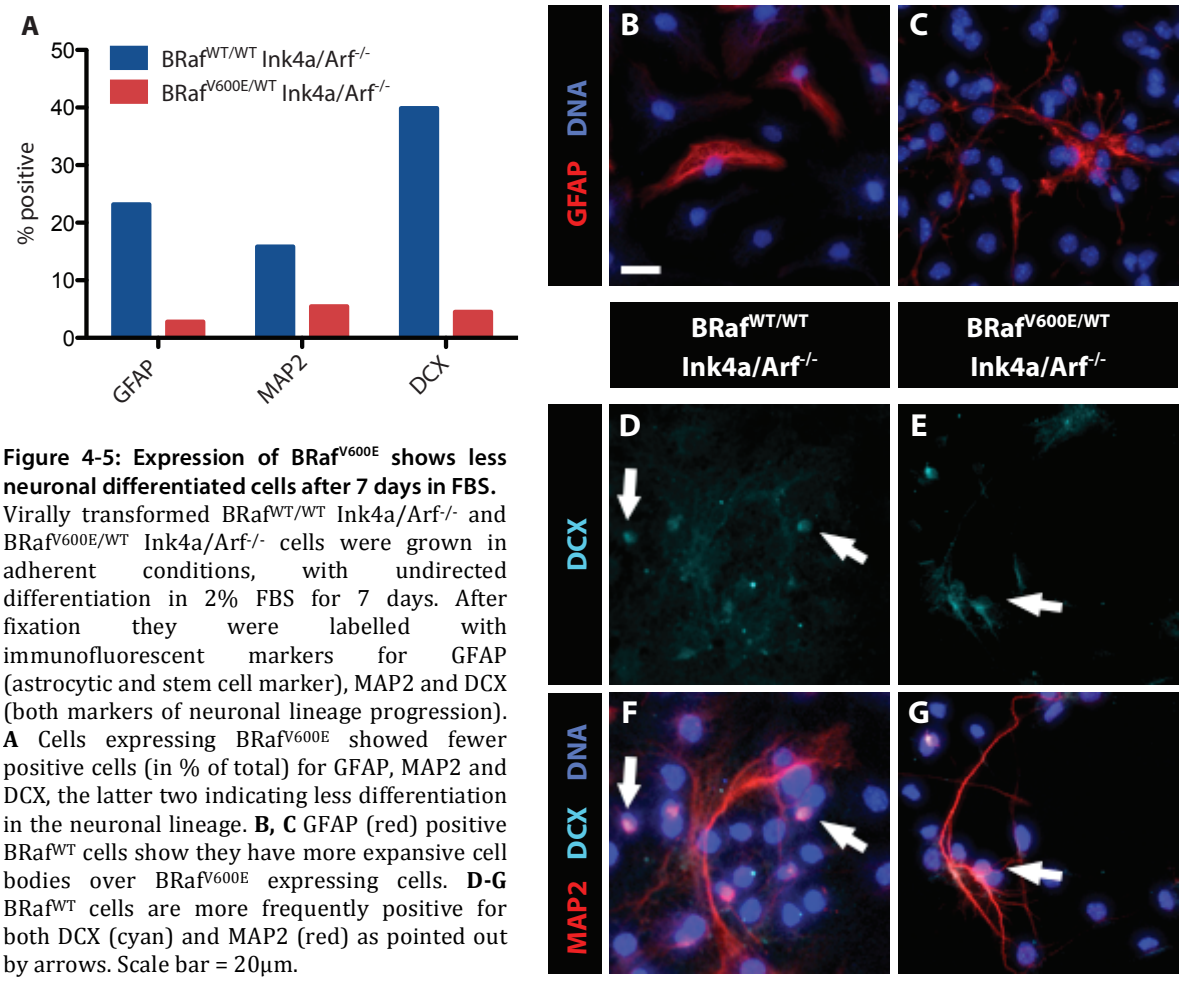

Figure 4-5: Expression of BRaf^{V600E} shows less neuronal differentiated cells after 7 days in FBS. Virally transformed BRaf$^{WT/WT}$ Ink4a/Arf$^{-/-}$ and BRaf$^{V600E/WT}$ Ink4a/Arf$^{-/-}$ cells were grown in adherent conditions, with undirected differentiation in 2% FBS for 7 days. After fixation they were labelled with immunofluorescent markers for GFAP (astrocytic and stem cell marker), MAP2 and DCX (both markers of neuronal lineage progression). **A** Cells expressing BRaf^{V600E} showed fewer positive cells (in % of total) for GFAP, MAP2 and DCX, the latter two indicating less differentiation in the neuronal lineage. **B, C** GFAP (red) positive BRaf^{WT} cells show they have more expansive cell bodies over BRaf^{V600E} expressing cells. **D-G** BRaf^{WT} cells are more frequently positive for both DCX (cyan) and MAP2 (red) as pointed out by arrows. Scale bar = 20µm.

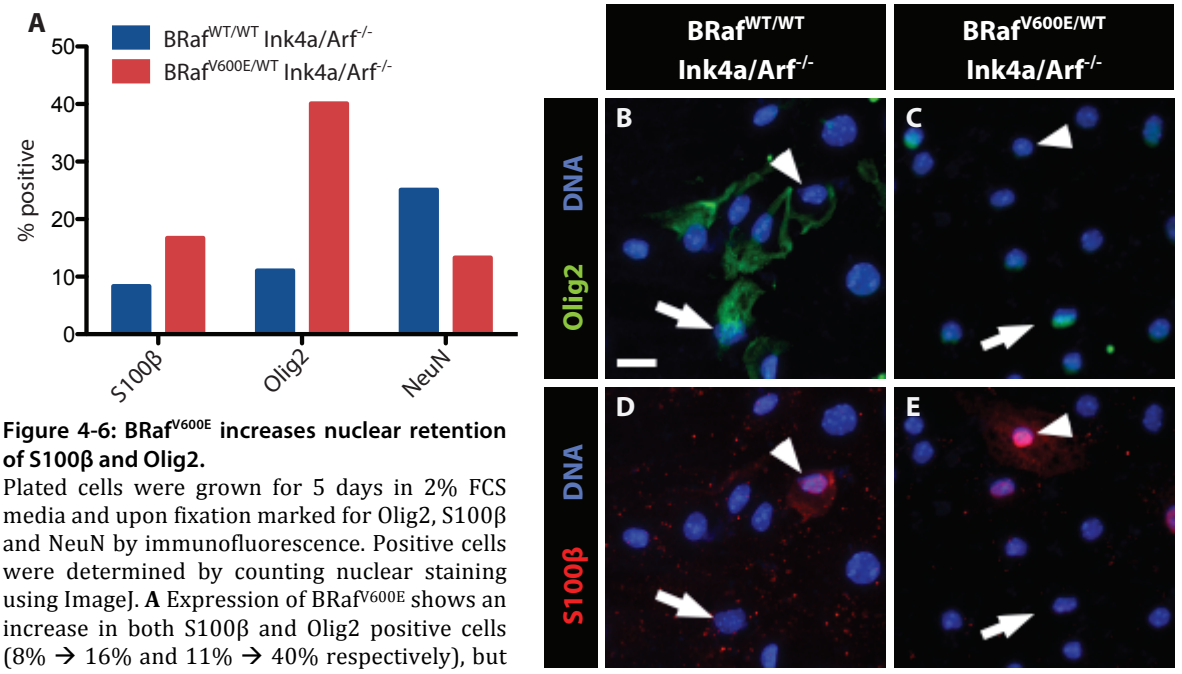

Figure 4-6: BRaf^{V600E} increases nuclear retention of S100β and Olig2. Plated cells were grown for 5 days in 2% FCS media and upon fixation marked for Olig2, S100β and NeuN by immunofluorescence. Positive cells were determined by counting nuclear staining using ImageJ. **A** Expression of BRaf^{V600E} shows an increase in both S100β and Olig2 positive cells (8% → 16% and 11% → 40% respectively), but decrease in NeuN (25% → 13%) compared to BRaf$^{WT/WT}$. **B, C** Olig2^{+} cells (green) are much more frequent and exhibit nuclear retention in BRaf$^{V600E/WT}$ Ink4a/Arf$^{-/-}$ (indicated by arrows), while in BRaf$^{WT/WT}$ Ink4a/Arf$^{-/-}$ cells Olig2 is also located in the cytoplasm. **D, E** BRaf^{V600E} expression increases frequency of cells positive for S100β (red, arrowheads). Cells positive for S100β were found negative for Olig2. Scale bar = 20µm.

BRaf^{V600E} expressing cells further showed an increase of relative intensity (a custom method to compare the relative level of cytoplasmic expression, see section 3.9) of Nestin, and decrease in Olig2 and GFAP (Figure 4-7A). The increase in Nestin (also seen in Figure 4-7B and C), S100β, nuclear Olig2 (see Figure 4-6A for both), and decrease in GFAP (seen in Figure 4-7D and E) in BRaf$^{V600E/WT}$ Ink4a/Arf$^{-/-}$ cells accompanied with the find of cytoplasmic Olig2 in BRaf$^{WT/WT}$ cells suggests the expression of BRaf^{V600E} either prevents maturation into astrocytes or delays differentiation of glial or oligodendrocyte progenitor cells.

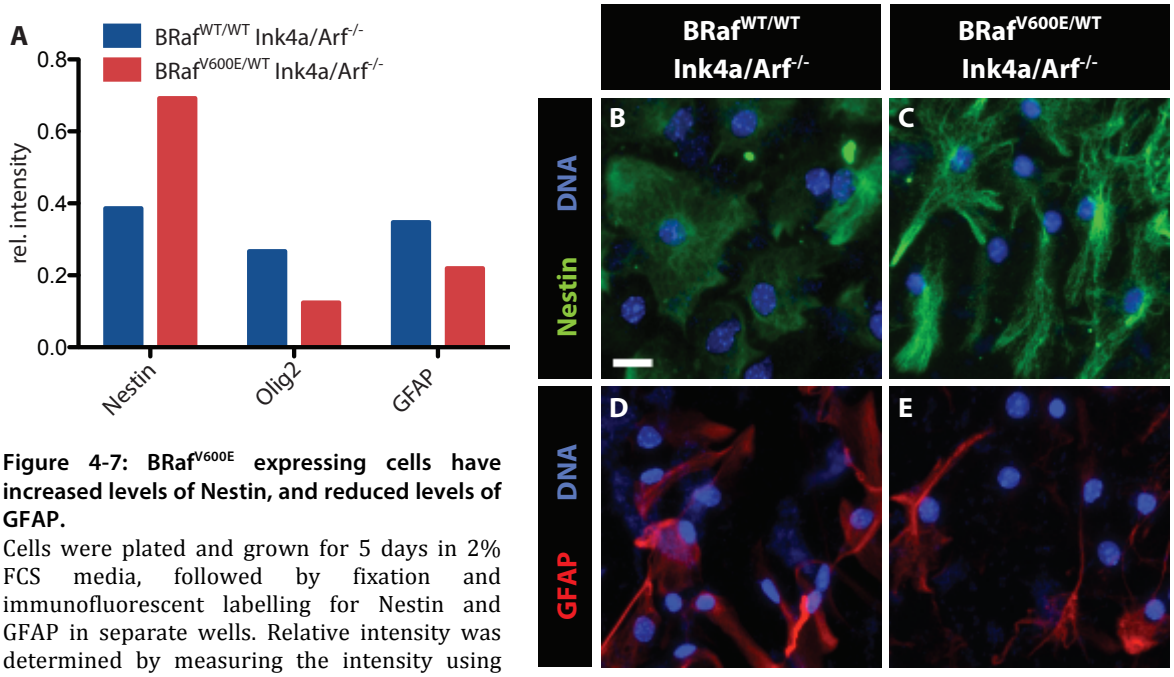

Figure 4-7: BRaf^{V600E} expressing cells have increased levels of Nestin, and reduced levels of GFAP.
Cells were plated and grown for 5 days in 2% FCS media, followed by fixation and immunofluorescent labelling for Nestin and GFAP in separate wells. Relative intensity was determined by measuring the intensity using ImageJ and dividing by the number of cells. **A** Expression of BRaf^{V600E} leads to an increase in relative intensity of Nestin (green; panels **B** and **C**), and a decrease of Olig2 (green; panels **B** and **C**) and GFAP (red; panels **D** and **E**). Scale bar = 20μm.

Nuclear export of the transcription factor Olig2 occurs during astrocyte differentiation and has been found dependant on phosphorylation by Akt (Setoguchi and Kondo, 2004). Furthermore, BRaf^{V600E} has been found to negatively regulate Akt in melanoma (Chen et al., 2012), but little is known about its mode of action in gliomas.

To determine if nuclear retention of Olig2 is indeed influenced by and can be reversed by blocking BRaf^{V600E} activity cells were grown in undirected differentiation media with PLX4720 or LY29004 (an inhibitor of PI3-Kinase specific activation of AKT) as positive control for 7 days.

BRaf$^{WT/WT}$ Ink4a/Arf$^{-/-}$ cells grown without either PLX4720 or LY29004 showed few positive for nuclear localised Olig2 (Figure 4-8A and B). Adding PLX4720 showed a slight rise in nuclear localised Olig2^{+} cells which were also GFAP^{-} (Figure 4-8A and C).

An increase in PLX4720 concentration only increased this phenotype (Figure 4-8A), which could be related to a possible activation of $BRaf^{WT}$ by PLX4720 (Hatzivassiliou et al., 2010). Treating with LY29004 leads to smaller cells, a further increase in nuclear retention of Olig2 and the percentage of nuclear Olig2 ($Olig2^n$) positive cells rose from 8% with vehicle to 20% with LY29004 (Figure 4-8C).

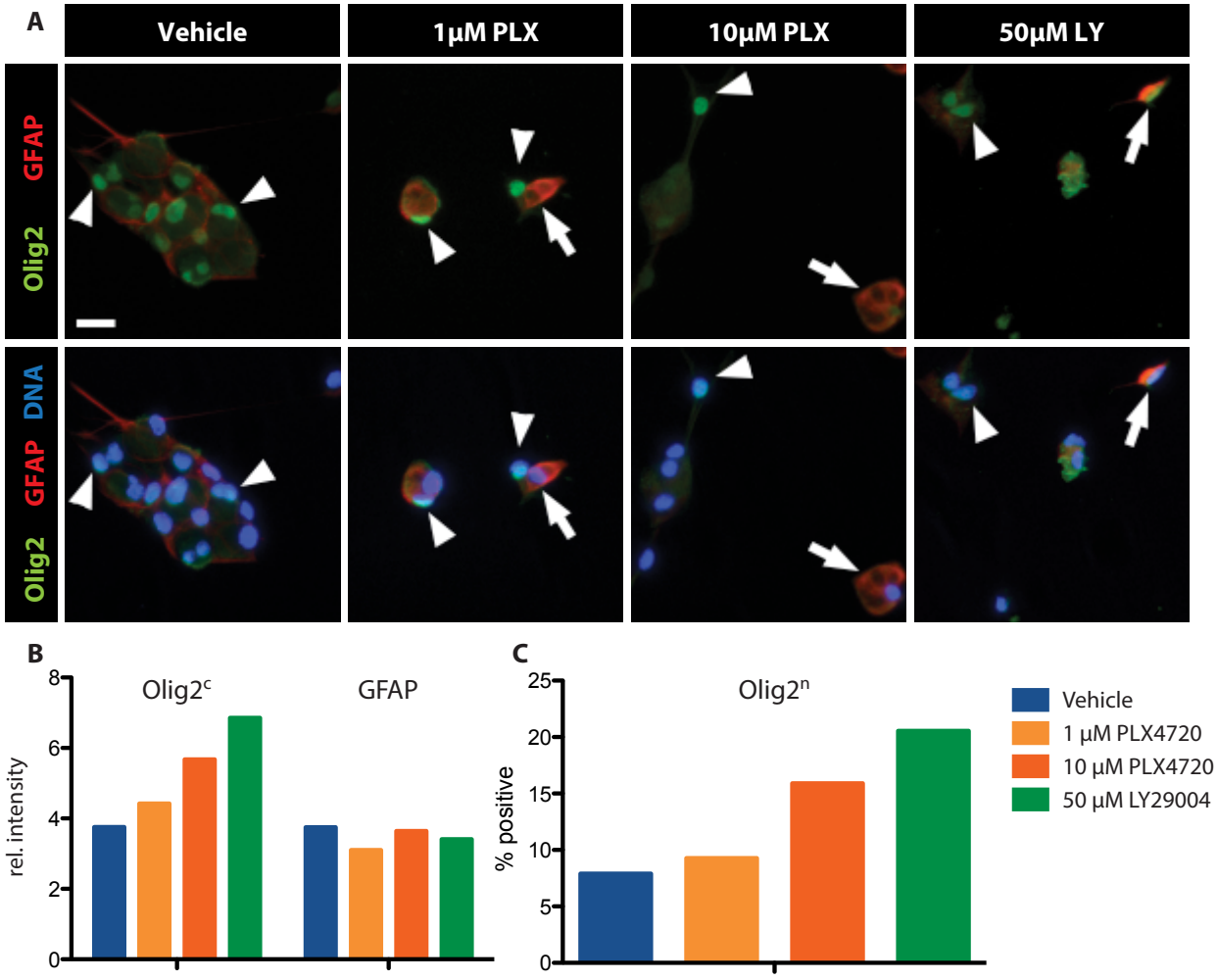

Figure 4-8: Treatment with PLX4720 induces nuclear phenotype in $BRaf^{WT/WT}$ Ink4a/$Arf^{-/-}$.
Cells were plated in DMSO (vehicle), 1 µM and 10 µM PLX4720 (PLX), and 50µM LY29004 (LY) and grown for 5 days under adherent conditions in 2% FCS media. **A** Increasing concentration of PLX4720 in $BRaf^{WT/WT}$ Ink4a/$Arf^{-/-}$ cells increases nuclear retention of Olig2 (green) (indicated by arrowheads) and leads to an altered morphology as indicated by cellular localisation of GFAP (red) (see Arrows). Treatment with AKT inhibitor LY29004 leads to further increased levels of nuclear retarded Olig2 and shrivelled-up cell bodies. **B** Relative intensity of Olig2 increases with increasing concentrations of PLX4720 and further increases after incubation with LY, the relative intensity of GFAP is comparable in these conditions. **C** Nuclear located Olig2 is found in 8% of cells grown in vehicle, increases with the addition of PLX4720 (9% and 16% for 1µM and 10µM of drug) and increases up to 20% when treated with LY29004. Scale bar = 20µm.

In contrast, two thirds of $BRaf^{V600E/WT}$ Ink4a/$Arf^{-/-}$ cells treated with vehicle had nuclear localised Olig2 (Figure 4-9C). Adding PLX4720 reduced nuclear retention of Olig2 (67% → 25%) and showed a change in morphology (Figure 4-9A and C), increasing the concentration of PLX4720 resulted in an increased intensity of GFAP (Figure 4-9B) and similar levels of nuclear Olig2 (Figure 4-9A and C). $BRaf^{V600E/WT}$

Ink4a/Arf$^{-/-}$ cells treated with LY29004 showed very little GFAP expression (Figure 4-9A) and a further reduced the percentage of nuclear Olig2+ cells to 6% (Figure 4-9C).

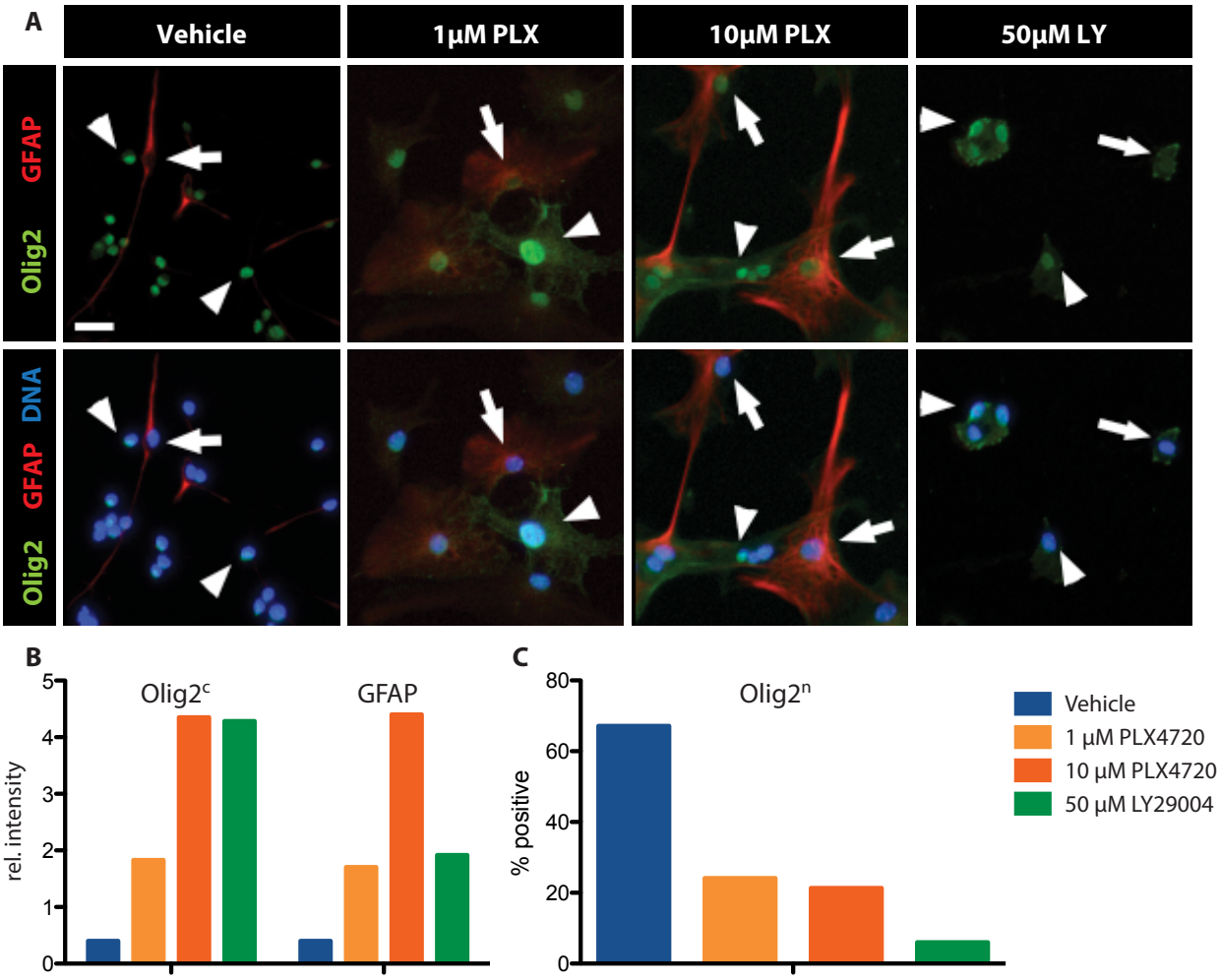

Figure 4-9: BRaf^{V600E} expressing cells export Olig2 when treatmed with PLX4720.
BRaf$^{V600E/WT}$ Ink4a/Arf$^{-/-}$ cells were plated in adherent conditions in media supplemented with 2% FCS, treated with DMSO, 1μM and 10μM PLX4720 and 50μM LY29004 and left to grow for 5 days. **A** Cells treated with PLX4720 show increased amount of GFAP (red) positive cells. These also have low levels of nuclear Olig2 (green) (see arrows). Cells with nuclear Olig2 show no expression of GFAP (see arrowheads). Treatment with AKT-inhibitor LY29004 yields several cells with cytoplasmic Olig2 (arrow), few with nuclear retarded Olig2 (arrowheads) and low levels of GFAP. **B** The relative intensities of Olig2 and GFAP increases with the concentration of PLX4720. Treatment with LY29004 shows similar relative intensity for Olig2 as treatment with 10μM PLX4720, but less than half the relative intensity of GFAP. **C** BRaf^{V600E} expressing cells treated with 1μM PLX4720 show a reduction in nuclear retention from 67% to 25%. Increased amount of drug shows only little change (25% → 21%), however, treatment with LY29004 results in almost exclusive export of Olig2 (6% nuclear retention). Scale bar = 20μm.

To determine the effect of BRaf^{V600E} on oligodendrocyte lineage progression specifically, cells were grown with oligodendrocyte promoting factors (triiodothyronine, T3, and insulin-like growth factor 1, IGF-1) for 10 days and stained for NSCs, TAPs, GRPs, OPCs, type-1 and type-2 astrocytes.

60% of BRaf^{V600E} expressing cells were found in OPC state, over 24% of BRaf^{WT}, as indicated by Olig2 (Figure 4-10A). Furthermore, BRaf^{V600E} expression also led to an increase in NSCs and TAPs (indicated by EGFR and CD15), and an increased relative intensity of GFAP, A2B5 and NG2 (Figure 4-10B) when compared with BRaf^{WT}, whereas

GFAP was accumulated in cell clusters and not more frequent than in BRaf$^{WT/WT}$ cells. Both BRaf$^{WT/WT}$ Ink4a/Arf$^{-/-}$ and BRaf$^{V600E/WT}$ Ink4a/Arf$^{-/-}$ cells were found as either GRPs/OPCs (A2B5^{+}/GFAP^{-}) or type-1 astrocytes (A2B5^{-}/GFAP^{+}), but not Type-2 astrocytes (A2B5^{+}/GFAP^{+}) (Figure 4-10C and 16D). BRaf$^{V600E/WT}$ Ink4a/Arf$^{-/-}$ cells differed noticeably in morphology and GFAP distribution, compared to BRaf$^{WT/WT}$ Ink4a/Arf$^{-/-}$, but in both cases were only found with nuclear Olig2, in GFAP negative cells (Figure 4-10E and 16F). BRaf$^{WT/WT}$ Ink4a/Arf$^{-/-}$ cells had fewer NG2 positive cells than the BRaf$^{V600E/WT}$ mutants, all of which were GFAP^{-} too (Figure 4-10G and H). Overall, expression of BRaf^{V600E} led to an increase in all used stem and progenitor cell markers and even after 10 days of oligodendrocyte promoting growth cells expressing GFAP did not morphologically resemble astrocytes.

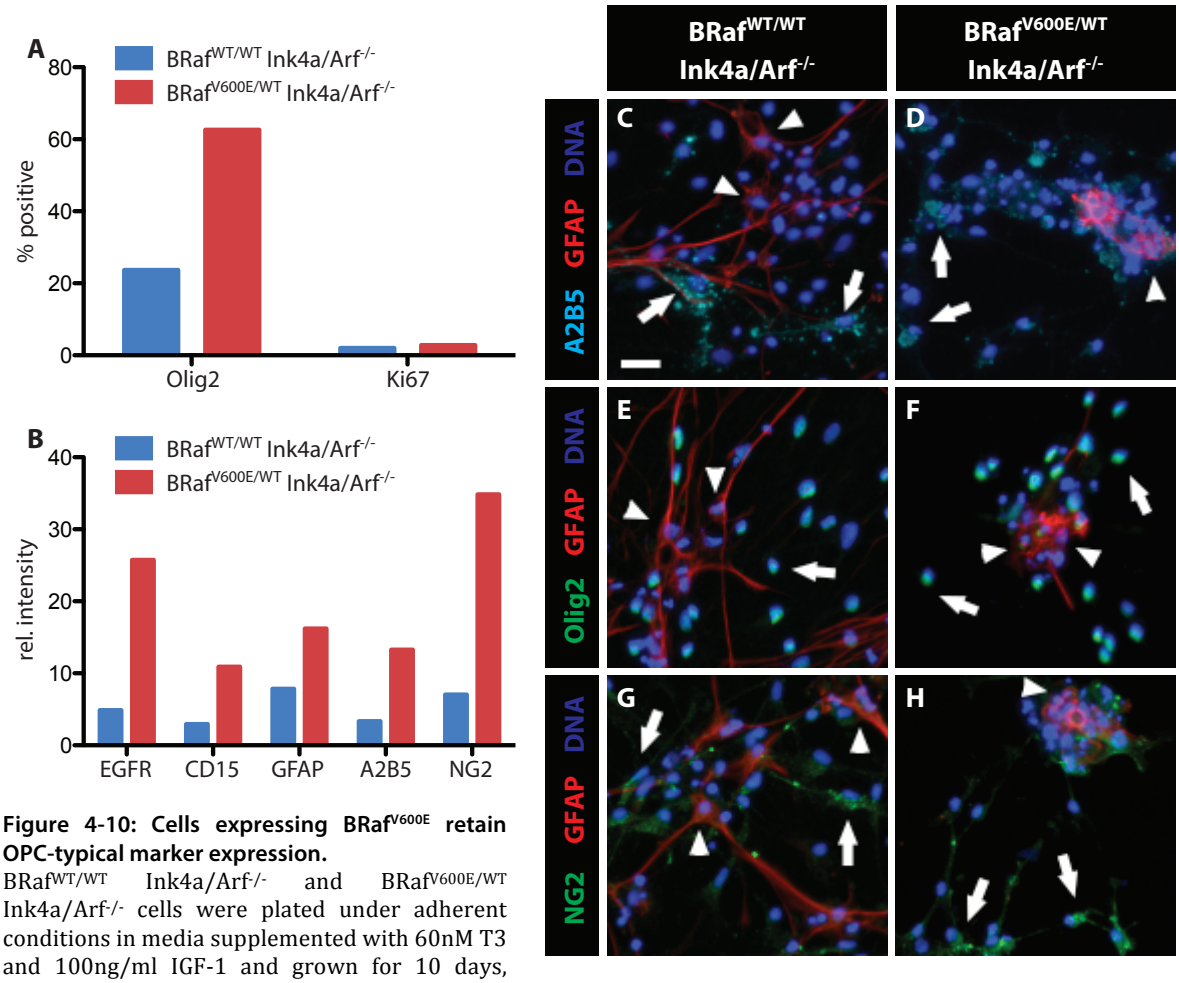

Figure 4-10: Cells expressing BRaf^{V600E} retain OPC-typical marker expression.
BRaf$^{WT/WT}$ Ink4a/Arf$^{-/-}$ and BRaf$^{V600E/WT}$ Ink4a/Arf$^{-/-}$ cells were plated under adherent conditions in media supplemented with 60nM T3 and 100ng/ml IGF-1 and grown for 10 days, supplementing media every 2. After fixation they were marked with Ki67/GFAP/A2B5, NG2/GFAP, Olig2/EGFR/CD15 and Olig2/GFAP. **A** Olig2 and K67 were counted as % of total cells using ImageJ. 62% of cells expressing BRaf^{V600E} and 24% of BRaf$^{WT/WT}$ Ink4a/Arf$^{-/-}$ cells were positive for Olig2, while in Ki67 it was 2% and 3% respectively. **B** Relative intensity was determined using a built-in function in ImageJ. Cells expressing BRaf^{V600E} had higher relative intensities for EGFR, CD15, GFAP, A2B5 and NG2, ranging from a 2-fold increase (in GFAP) to a 5-fold increase (EGFR and NG2). **C, D** A2B5 (cyan; arrows) positive cells are GFAP (red; arrowheads) negative. **E, F** Both BRaf$^{WT/WT}$ Ink4a/Arf$^{-/-}$ and BRaf$^{V600E/WT}$ Ink4a/Arf$^{-/-}$ cells present Olig2 (green) in the nucleus (arrows), and GFAP^{+} (red) cells (arrowheads) are also Olig2^{-}. Olig2^{+} cells are also more frequent in presence of BRaf^{V600E} expression. **G, H** NG2 (green) is localised in the cell membrane of GFAP^{-} cells (arrows) and can be found more frequently in BRaf^{V600E} expressing cells. GFAP^{+}/NG2^{-} cells are marked with arrowheads. **C-H** GFAP expression is found at a higher intensity, but in much fewer cells under BRaf^{V600E} than in BRaf^{WT} cells. Scale bar = 20µm.

4.3 BRaf^{V600E} expressing neurospheres divide more symmetrically

Cellular localisation of cell fate determinants is essential for asymmetric cell division in D. melanogaster neuroblasts as much as vertebrate NSCs (Bultje et al., 2009; Lee et al., 2006). Furthermore, it has been suggested, that stem and progenitor cells defective for ACD initiate tumours (Caussinus and Gonzalez, 2005; Morrison and Kimble, 2006). It is currently unknown, if BRaf^{V600E} changes asymmetric cell division and at which lineage stage this occurs.

To determine if expression of BRaf^{V600E} influences asymmetric cell division, I used a pair assay to visualise the asymmetric division of neural stem cells (marked by Mash1), transit amplifying cells (marked by EGFR and CD15), and OPCs (marked by Olig2). Par-3, an adaptor protein involved in the tight junction during asymmetric cell division, served as a positive control. Single asymmetry values for each marker were measured (Figure 4-11A) and compared independently. TAP and OPC markers showed a decreased asymmetric distribution under expression of BRaf^{V600E} (Figure 4-11B).

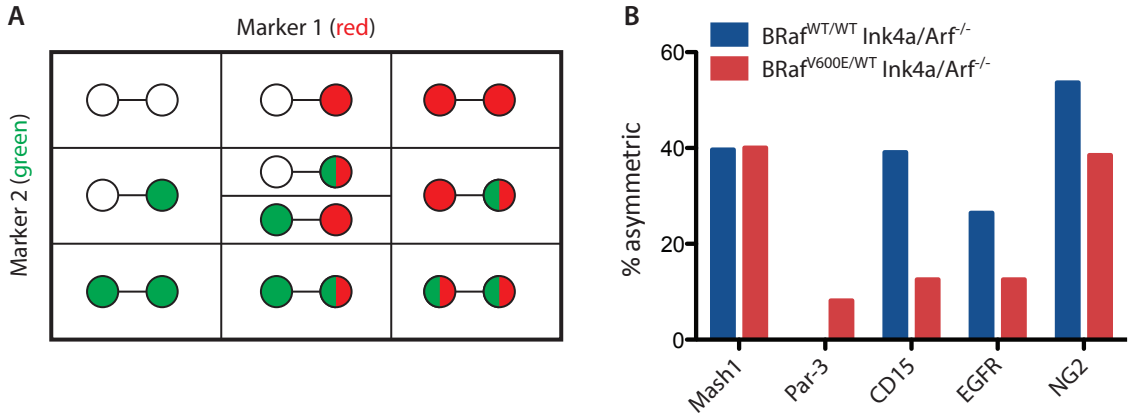

Figure 4-11: Expression of BRaf^{V600E} leads to decreased asymmetry in NSC markers.
A Status of symmetry and asymmetry was recorded in all possibilities as indicated schematically. Further references of asymmetry focus on the single marker distribution, as seen in second row and column. **B** Cells expressing BRaf^{V600E} exhibited a decreased asymmetry (and by association increase in symmetric distribution) of CD15 (39% -> 12%), EGFR (26% -> 12%) and NG2 (54% -> 34%), an increase of asymmetry in Par-3 (0% -> 8%) and no change in distribution of Mash1.

Specific inhibition of BRaf^{V600E} with PLX4720 was used to determine if this effect is reversible. Chemical blocking of BRaf^{V600E} showed a restoration of asymmetric distribution for CD15 (Figure 4-12A). Interestingly, addition of PLX4720 led to an increase of symmetric NG2 distribution for both BRaf$^{WT/WT}$ Ink4a/Arf$^{-/-}$ and BRaf$^{V600E/WT}$ Ink4a/Arf$^{-/-}$ cells (Figure 4-12B). EGFR distribution saw a reduction in asymmetry (20% to 14%) in BRaf^{V600E} expressing cells upon PLX4720 treatment (Figure 4-12C). Markers

used were clearly distinguishable in either symmetric or asymmetric distribution and counted manually (Figure 4-12D).

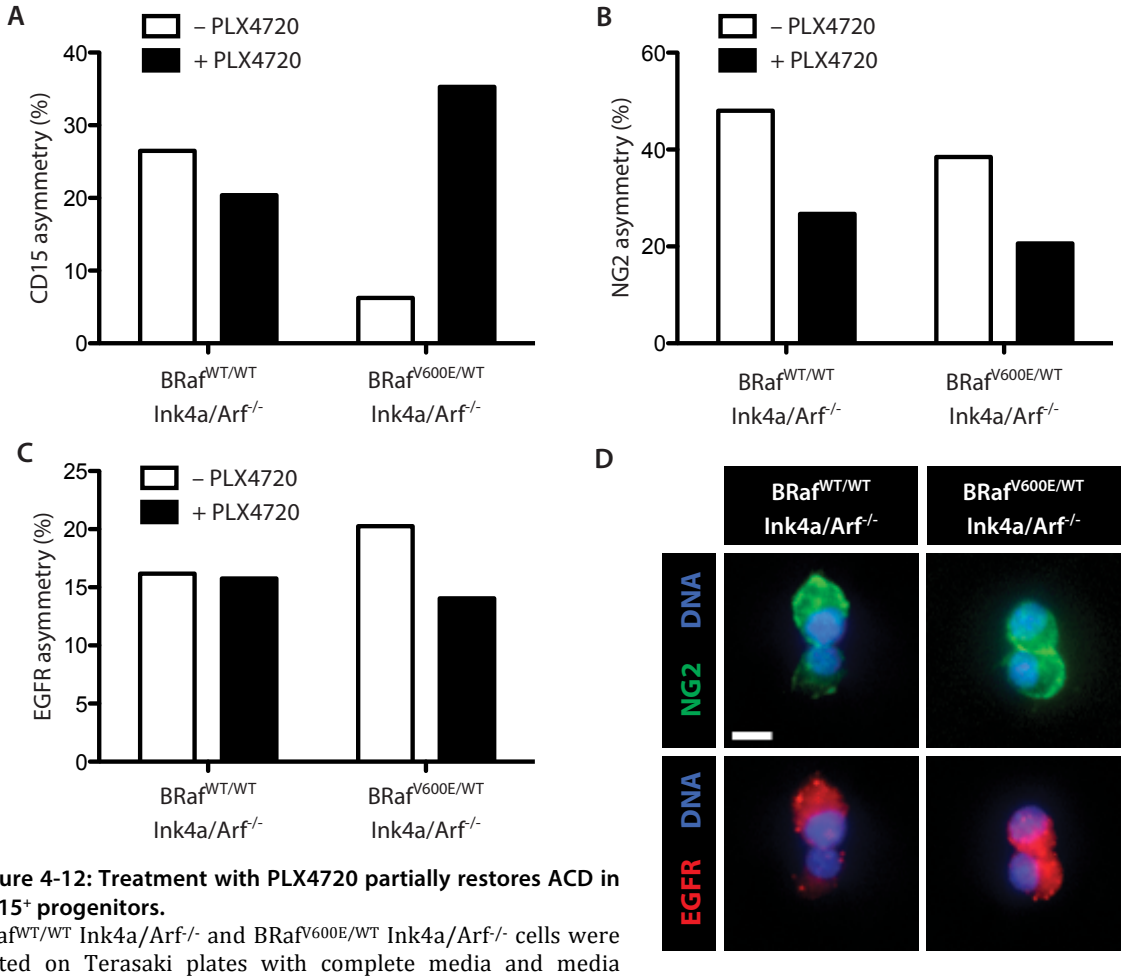

Figure 4-12: Treatment with PLX4720 partially restores ACD in CD15⁺ progenitors.
BRaf$^{WT/WT}$ Ink4a/Arf$^{-/-}$ and BRaf$^{V600E/WT}$ Ink4a/Arf$^{-/-}$ cells were plated on Terasaki plates with complete media and media containing 1μM PLX4720 and were grown until daughter cells could be observed (16-24 hours). **A** In BRaf^{V600E} expressing cells PLX4720 treatment showed a restoration of CD15 asymmetry levels to the BRaf$^{WT/WT}$ range (6% to 35%) and a decrease in BRaf$^{WT/WT}$ Ink4a/Arf$^{-/-}$ (26% to 20%). **B** Asymmetric distribution of Par-3 was increased in both wild type and BRaf$^{V600E/WT}$ Ink4a/Arf$^{-/-}$ cells (0% to 17% and 8% to 24% respectively). **C** NG2 asymmetry was reduced in both cell lines upon PLX4720 treatment (48% to 26% for wild type and 38% to 20% for BRaf$^{V600E/WT}$ Ink4a/Arf$^{-/-}$). **D** Addition of PLX4720 had no effect on EGFR distribution in BRaf$^{WT/WT}$ Ink4a/Arf$^{-/-}$ cells (16% to 15.75%) and reduced asymmetry in cells expressing BRaf^{V600E}. **E, G** Asymmetry and **F-H** symmetry was determined by microscopic analysis and manually counting. Cells depicted here were stained for NG2 (green), EGFR (red) and DNA (blue). Scale bar = 10μm.

5 Discussion

5.1 Combination treatment of erlotinib and vemurafenib could confer an increased benefit for patients over single treatment.

EGFR signalling is extensive and has been widely researched. It stimulates the Ras/Raf/MEK/ERK, PI3K/Akt and JNK pathways to signal growth, survival and differentiation and is often found highly expressed or mutated in various cancers (Oda et al., 2005; Salomon et al., 1995). Furthermore, EGFR overexpression is also found in 50% of grade IV gliomas, glioblastoma multiforme. This prevalence makes it an attractive target for inhibition and has led to the development of the small molecule inhibitors gefitinib (Iressa) and erlotinib (Tarceva), which are ATP competitors, originally approved for the treatment of non-small cell lung cancer and in clinical trials for treatment of glioblastoma.

While initially promising recent research in to erlotinib treatment have shown mixed results. A phase I/II clinical study of an erlotinib, radiotherapy and TMZ combination treatment in GBM patients, some of which (37%) had the amplified variant EGFRvIII, showed this treatment provided no benefit to the cohort presenting EGFR amplification (Brown et al., 2008). Furthermore, it has been shown that patients with high levels of EGFR expression and high levels of Akt phosphorylation respond worse to erlotinib, than those with low Akt phosphorylation (Haas-Kogan et al., 2005). A recent erlotinib dose escalation study shows that erlotinib toxicity took a toll on the patients before they could benefit from its therapy (Kesavabhotla et al., 2012). Finally, Prados et al. (2009) shows a statistically significant increase in treatment with a similar regimen to Brown et al., 2008, but only conferred a progression free survival of 8.2 months, over 4.9 months (or a median survival of 19.3 months, over 14.1 months) with placebo. While scientifically significant Prados et al. recorded 43 severe, and 5 life-threatening adverse events in 66 patients. In summary erlotinib continues to show disappointing clinical benefit for patients, however when combined with other treatments can show better results than alone.

Similarly, inhibitors for the commonly found mutated $BRaf^{V600E}$ are under development. The first $BRaf^{V600E}$-specific drug vemurafenib (PLX4032, marketed as Zelboraf) has been approved for treatment of late-stage melanoma and in early clinical trials has shown up to 80% response to treatment (Flaherty et al., 2010). In addition,

vemurafenib has been shown to reduce proliferation on human glioma tumour cell lines and brain xenografts positive for $BRaf^{V600E}$ (Nicolaides et al., 2011), but has not yet been tested in clinical trials. Treatment with vemurafenib, however, still needs further research, as it has also been found to activate $BRaf^{WT}$ (Halaban et al., 2010).

Previous research indicates, that vemurafenib treatment can lead to activated MAPK signalling and growth in $BRaf^{WT}$-melanoma that are also carrying an activating KRAS mutation (Hatzivassiliou et al., 2010). The initial publication highlighting the selectivity of vemurafenib pointed out it also binds to $BRaf^{WT}$, but does so at a 10-fold lower specificity, than to $BRaf^{V600E}$ (Tsai et al., 2008). Hatzivassiliou et al. suggest, this binding leads to a conformational change leading to heterodimerisation of c-Raf with BRaf. Similarly, Heidorn et al. (2010) show this interaction is mediated by oncogenic Ras, which could also suggest similar effects by RTK signalling, which also activates Ras.

In summary, while vemurafenib is effective against $BRaf^{V600E}$ combination treatment with erlotinib potently inhibits proliferation of $BRaf^{WT}$ Ink4a/$Arf^{-/-}$ cells *in vitro*. This combination treatment could potentially counteract vemurafenib-mediated $BRaf^{WT}$ activation in non-tumour cells. These or other combinations, however remain an issue for future research.

5.2 Expression of $BRaf^{V600E}$ retains oligodendrocyte progenitor phenotype through regulation of Akt

The basic helix-loop-helix transcription factor Olig2 has been shown to be a key regulator of oligodendrocyte and astrocyte differentiation {Takebayashi:2002tx}. Most notably, it is found expressed in OPCs and promotes oligodendrocyte differentiation, but when absent OPCs undergo astrocyte differentiation {Takebayashi:2000wi, Zhou:2002ux}. Moreover, Olig2 has been observed to undergo nuclear export in OPCs following brain injury, and in the process generate astrocytes {Magnus:2007jl}. This process has been suggested to be dependant on Akt-mediated Olig2 phosphorylation {Setoguchi:2004js}.

Based on the observation that $BRaf^{V600E}$ leads to increased proliferation and the cells continue to form neurospheres in vitro the differentiation assay focused on glial restricted and O2A progenitors. The results presented in this thesis suggest treatment with PLX4720 restores normal neuronal and oligodendrocyte differentiation in cells expressing $BRaf^{V600E}$. Nuclear export of Olig2 in these cells could be inhibited through $BRaf^{V600E}$-mediated Akt inactivation, which has been shown to occur in melanoma cells

in an mTORC2-dependant manner {Chen:2012di}. Furthermore, my results suggest treatment with PLX4720 could lead to an increase in OPCs in $BRaf^{WT}$ expressing cells. If this is the case, it might be regulated through the previously described $BRaf^{WT}$-vemurafenib-c-Raf heterodimers, however knockdown of c-Raf in both $BRaf^{WT}$ and $BRaf^{V600E}$ expressing cells has so far been shown to not impact Akt phosphorylation {Chen:2012di}.

Further analysis regarding the mechanistic regulation of oligodendrocyte and astrocyte differentiation, however, remains a matter of further research.

5.3 $BRaf^{V600E}$ promotes expansion of neural stem cells and glial restricted progenitors

NSCs isolated from the adult subventricular zone have been shown to express CD15 (also known as Lewis X, SSEA-1) and release it into their environment (Capela and Temple, 2002). These cells have been found to further differentiate following asymmetric distribution of EGFR, leading to cells of different fate: $EGFR^{low}$/$Olig2^{+}$ late glial restricted/early oligodendrocyte progenitors and $EGFR^{high}$/$RC2^{+}$ transit amplifying cells (Sun et al., 2005). Furthermore, our lab has previously shown, that cells expressing the constitutively active EGFR mutant *verbB* have asymmetry defects and orthotopically injected *verbB*/$NG2^{+}$ OPCs can initiate tumours reminiscent of oligodendroglioma (Sugiarto et al., 2011). This data and previous results suggesting that cells expressing $BRaf^{V600E}$ remain progenitor cells led to investigating if $BRaf^{V600E}$ also influences asymmetric cell division (ACD).

In *Drosophila* neuroblasts defects in ACD have been clearly shown to lead to cancer {Lee:2006hq}, this is thought to occur in mammalian cells too, but their ACD machinery is much more complex. In contrast to *Drosophila* neuroblasts, asymmetric cell division in developing mammalian brain is thought to involve not only the Par3/Par6/aPKC complex, but also the orientation of the cleavage plane {Kosodo:2004js}. Recently, it has been demonstrated in mice, that in oblique divisions (occurring at ~45°), Par3 regulates Notch and regulates cell fate {Bultje:2009ez}. While MAPK signalling both through mutant EGFR and BRaf has been shown to result in ACD defects the mechanistic link is unknown.

The results presented in this thesis show that NSCs and transit amplifying cells have an increased capacity to self-renew when expressing $BRaf^{V600E}$ and this behaviour

can be reversed by inhibition with by specifically blocking $BRaf^{V600E}$. Furthermore the expression of $BRaf^{V600E}$ leads to asymmetry defects in NSCs and retains cells in oligodendrocyte progenitor status.

However, which cell type the resulting tumours arise from needs to be further investigated. It has been shown that oncogenes can lead to dedifferentiation of mature astrocytes and neurons which then leads to gliomas {FriedmannMorvinski:2012hb}. Equally, neural stem and progenitor cells have been shown to lead to gliomas too {Bachoo:2002wi, Sugiarto:2011ee}. Understanding how and which cells gliomas arise from remains an important issue. The gained insight will allow us to classify gliomas more accurately by genetics as well as histology and could provide more accurate markers for earlier diagnosis. Finally, we would also be able to offer better treatments and might even be able to predict or even prevent recurrence.

6 Bibliography

Aguirre, A.J., Bardeesy, N., Sinha, M., Lopez, L., Tuveson, D.A., Horner, J., Redston, M.S., and DePinho, R.A. (2003). Activated Kras and Ink4a/Arf deficiency cooperate to produce metastatic pancreatic ductal adenocarcinoma. Genes Dev. 17, 3112–3126.

Atwood, S.X., and Prehoda, K.E. (2009). aPKC phosphorylates Miranda to polarize fate determinants during neuroblast asymmetric cell division. Curr. Biol. 19, 723–729.

Bachoo, R.M., Maher, E.A., Ligon, K.L., Sharpless, N.E., Chan, S.S., You, M.J., Tang, Y., DeFrances, J., Stover, E., Weissleder, R., et al. (2002). Epidermal growth factor receptor and Ink4a/Arf: convergent mechanisms governing terminal differentiation and transformation along the neural stem cell to astrocyte axis. Cancer Cell 1, 269–277.

Barnier, J.V., Papin, C., Eychène, A., Lecoq, O., and Calothy, G. (1995). The mouse B-raf gene encodes multiple protein isoforms with tissue-specific expression. J. Biol. Chem. 270, 23381–23389.

Berdnik, D., Török, T., González-Gaitán, M., and Knoblich, J.A. (2002). The endocytic protein alpha-Adaptin is required for numb-mediated asymmetric cell division in Drosophila. Dev. Cell 3, 221–231.

Blalock, W.L., Weinstein-Oppenheimer, C., Chang, F., Hoyle, P.E., Wang, X.Y., Algate, P.A., Franklin, R.A., Oberhaus, S.M., Steelman, L.S., and McCubrey, J.A. (1999). Signal transduction, cell cycle regulatory, and anti-apoptotic pathways regulated by IL-3 in hematopoietic cells: possible sites for intervention with anti-neoplastic drugs. Leukemia 13, 1109–1166.

Bollag, G., Hirth, P., Tsai, J., Zhang, J., Ibrahim, P.N., Cho, H., Spevak, W., Zhang, C., Zhang, Y., Habets, G., et al. (2010). Clinical efficacy of a RAF inhibitor needs broad target blockade in BRAF-mutant melanoma. Nature 467, 596–599.

Brown, P.D., Krishnan, S., Sarkaria, J.N., Wu, W., Jaeckle, K.A., Uhm, J.H., Geoffroy, F.J., Arusell, R., Kitange, G., Jenkins, R.B., et al. (2008). Phase I/II trial of erlotinib and temozolomide with radiation therapy in the treatment of newly diagnosed glioblastoma multiforme: North Central Cancer Treatment Group Study N0177. J. Clin. Oncol. 26, 5603–5609.

Bultje, R.S., Castaneda-Castellanos, D.R., Jan, L.Y., Jan, Y.N., Kriegstein, A.R., and Shi, S.-H. (2009). Mammalian Par3 regulates progenitor cell asymmetric division via notch signaling in the developing neocortex. Neuron 63, 189–202.

Cameron, H.A., and Gould, E. (1996). Distinct populations of cells in the adult dentate gyrus undergo mitosis or apoptosis in response to adrenalectomy. J. Comp. Neurol. 369, 56–63.

Capela, A., and Temple, S. (2002). LeX/ssea-1 is expressed by adult mouse CNS stem cells, identifying them as nonependymal. Neuron 35, 865–875.

Caussinus, E., and Gonzalez, C. (2005). Induction of tumor growth by altered stem-cell asymmetric division in Drosophila melanogaster. Nat. Genet. 37, 1125–1129.

Chang, F., Steelman, L.S., Lee, J.T., Shelton, J.G., Navolanic, P.M., Blalock, W.L., Franklin, R.A., and McCubrey, J.A. (2003). Signal transduction mediated by the Ras/Raf/MEK/ERK pathway from cytokine receptors to transcription factors: potential targeting for therapeutic intervention. Leukemia 17, 1263–1293.

Chapman, P.B., Hauschild, A., Robert, C., Haanen, J.B., Ascierto, P., Larkin, J., Dummer, R., Garbe, C., Testori, A., Maio, M., et al. (2011). Improved survival with vemurafenib in melanoma with BRAF V600E mutation. N. Engl. J. Med. 364, 2507–2516.

Chen, B., Tardell, C., Higgins, B., Packman, K., Boylan, J.F., and Niu, H. (2012). BRAFV600E negatively regulates the AKT pathway in melanoma cell lines. PLoS ONE 7, e42598.

Choksi, S.P., Southall, T.D., Bossing, T., Edoff, K., de Wit, E., Fischer, B.E., van Steensel, B., Micklem, G., and Brand, A.H. (2006). Prospero Acts as a Binary Switch between Self-Renewal and Differentiation in Drosophila Neural Stem Cells. Dev. Cell 11, 775–789.

Dankort, D., Filenova, E., Collado, M., Serrano, M., Jones, K., and McMahon, M. (2007). A new mouse model to explore the initiation, progression, and therapy of BRAFV600E-induced lung tumors. Genes Dev. 21, 379–384.

Davies, H., Bignell, G.R., Cox, C., Stephens, P., Edkins, S., Clegg, S., Teague, J., Woffendin, H., Garnett, M.J., Bottomley, W., et al. (2002). Mutations of the BRAF gene in human cancer. Nature 417, 949–954.

Doetsch, F., Caillé, I., Lim, D.A., García-Verdugo, J.M., and Alvarez-Buylla, A. (1999). Subventricular Zone Astrocytes Are Neural Stem Cells in the Adult Mammalian Brain. Cell 97, 703–716.

Dolecek, T.A., Propp, J.M., Stroup, N.E., and Kruchko, C. (2012). CBTRUS Statistical Report: Primary Brain and Central Nervous System Tumors Diagnosed in the United States in 2005-2009. Neuro-Oncology 14, v1–v49.

Etemad-Moghadam, B., Guo, S., and Kemphues, K.J. (1995). Asymmetrically distributed PAR-3 protein contributes to cell polarity and spindle alignment in early C. elegans embryos. Cell 83, 743–752.

Flaherty, K.T., Puzanov, I., Kim, K.B., Ribas, A., McArthur, G.A., Sosman, J.A., O'Dwyer, P.J., Lee, R.J., Grippo, J.F., Nolop, K., et al. (2010). Inhibition of mutated, activated BRAF in metastatic melanoma. N. Engl. J. Med. 363, 809–819.

Gage, F.H. (2000). Mammalian neural stem cells. Science 287, 1433–1438.

Galabova-Kovacs, G., Catalanotti, F., Matzen, D., Reyes, G.X., Zezula, J., Herbst, R., Silva, A., Walter, I., and Baccarini, M. (2008). Essential role of B-Raf in oligodendrocyte maturation and myelination during postnatal central nervous system development. J. Cell Biol. 180, 947–955.

Glover, K.Y., Perez-Soler, R., and Papadimitradopoulou, V.A. (2004). A review of small-

molecule epidermal growth factor receptor-specific tyrosine kinase inhibitors in development for non-small cell lung cancer. Semin. Oncol. 31, 83–92.

Gregori, N., Pröschel, C., Noble, M., and Mayer-Pröschel, M. (2002). The tripotential glial-restricted precursor (GRP) cell and glial development in the spinal cord: generation of bipotential oligodendrocyte-type-2 astrocyte progenitor cells and dorsal-ventral differences in GRP cell function. J. Neurosci. 22, 248–256.

Haas-Kogan, D.A., Prados, M.D., Tihan, T., Eberhard, D.A., Jelluma, N., Arvold, N.D., Baumber, R., Lamborn, K.R., Kapadia, A., Malec, M., et al. (2005). Epidermal growth factor receptor, protein kinase B/Akt, and glioma response to erlotinib. J. Natl. Cancer Inst. 97, 880–887.

Hachem, S., Aguirre, A., Vives, V., Marks, A., Gallo, V., and Legraverend, C. (2005). Spatial and temporal expression of S100B in cells of oligodendrocyte lineage. Glia 51, 81–97.

Halaban, R., Zhang, W., Bacchiocchi, A., Cheng, E., Parisi, F., Ariyan, S., Krauthammer, M., McCusker, J.P., Kluger, Y., and Sznol, M. (2010). PLX4032, a selective BRAF(V600E) kinase inhibitor, activates the ERK pathway and enhances cell migration and proliferation of BRAF melanoma cells. Pigment Cell Melanoma Res 23, 190–200.

Hatzivassiliou, G., Song, K., Yen, I., Brandhuber, B.J., Anderson, D.J., Alvarado, R., Ludlam, M.J.C., Stokoe, D., Gloor, S.L., Vigers, G., et al. (2010). RAF inhibitors prime wild-type RAF to activate the MAPK pathway and enhance growth. Nature 464, 431–435.

Heidorn, S.J., Milagre, C., Whittaker, S., Nourry, A., Niculescu-Duvas, I., Dhomen, N., Hussain, J., Reis-Filho, J.S., Springer, C.J., Pritchard, C., et al. (2010). Kinase-dead BRAF and oncogenic RAS cooperate to drive tumor progression through CRAF. Cell 140, 209–221.

Horbinski, C., Hamilton, R.L., Nikiforov, Y., and Pollack, I.F. (2010). Association of molecular alterations, including BRAF, with biology and outcome in pilocytic astrocytomas. Acta Neuropathol. 119, 641–649.

Howlader, N., Noone, A.M., Krapcho, M., Garshell, J., Neyman, N., Altekruse, S.F., Kosary, C.L., Yu, M., Ruhl, J., Tatalovich, Z., et al. (2013). SEER Cancer Statistics Review, 1975-2006, National Cancer Institute. Bethesda, MD.

Hung, T.J., and Kemphues, K.J. (1999). PAR-6 is a conserved PDZ domain-containing protein that colocalizes with PAR-3 in Caenorhabditis elegans embryos. Development 126, 127–135.

Ivkovic, S., Canoll, P., and Goldman, J.E. (2008). Constitutive EGFR signaling in oligodendrocyte progenitors leads to diffuse hyperplasia in postnatal white matter. J. Neurosci. 28, 914–922.

Jacob, K., Quang-Khuong, D.-A., Jones, D.T.W., Witt, H., Lambert, S., Albrecht, S., Witt, O., Vezina, C., Shirinian, M., Faury, D., et al. (2011). Genetic aberrations leading to MAPK pathway activation mediate oncogene-induced senescence in sporadic pilocytic astrocytomas. Clin. Cancer Res. 17, 4650–4660.

Jones, D.T.W., Kocialkowski, S., Liu, L., Pearson, D.M., Bäcklund, L.M., Ichimura, K., and Collins, V.P. (2008). Tandem duplication producing a novel oncogenic BRAF fusion gene defines the majority of pilocytic astrocytomas. Cancer Res. 68, 8673–8677.

Kemphues, K.J., Priess, J.R., Morton, D.G., and Cheng, N.S. (1988). Identification of genes required for cytoplasmic localization in early C. elegans embryos. Cell 52, 311–320.

Kennea, N.L., and Mehmet, H. (2002). Neural stem cells. J. Pathol. 197, 536–550.

Kesavabhotla, K., Schlaff, C.D., Shin, B., Mubita, L., Kaplan, R., Tsiouris, A.J., Pannullo, S.C., Christos, P., Lavi, E., Scheff, R., et al. (2012). Phase I/II study of oral erlotinib for treatment of relapsed/refractory glioblastoma multiforme and anaplastic astrocytoma. J. Exp. Ther. Oncol. 10, 71–81.

Knoblich, J.A. (2010). Asymmetric cell division: recent developments and their implications for tumour biology. Nat. Rev. Mol. Cell Biol. 11, 849–860.

Lee, C.-Y., Robinson, K.J., and Doe, C.Q. (2006). Lgl, Pins and aPKC regulate neuroblast self-renewal versus differentiation. Nature 439, 594–598.

Ligon, K.L., Huillard, E., Mehta, S., Kesari, S., Liu, H., Alberta, J.A., Bachoo, R.M., Kane, M., Louis, D.N., DePinho, R.A., et al. (2007). Olig2-regulated lineage-restricted pathway controls replication competence in neural stem cells and malignant glioma. Neuron 53, 503–517.

Lois, C., and Alvarez-Buylla, A. (1994). Long-distance neuronal migration in the adult mammalian brain. Science 264, 1145–1148.

Louis, D.N., Ohgaki, H., Wiestler, O.D., Cavenee, W.K., Burger, P.C., Jouvet, A., Scheithauer, B.W., and Kleihues, P. (2007). The 2007 WHO classification of tumours of the central nervous system. Acta Neuropathol. 114, 97–109.

Lu, B., Ackerman, L., Jan, L.Y., and Jan, Y.N. (1999). Modes of protein movement that lead to the asymmetric localization of partner of Numb during Drosophila neuroblast division. Mol. Cell 4, 883–891.

Magnus, T., Coksaygan, T., Korn, T., Xue, H., Arumugam, T.V., Mughal, M.R., Eckley, D.M., Tang, S.-C., Detolla, L., Rao, M.S., et al. (2007). Evidence that nucleocytoplasmic Olig2 translocation mediates brain-injury-induced differentiation of glial precursors to astrocytes. J. Neurosci. Res. 85, 2126–2137.

Mao, X.-G., Zhang, X., Xue, X.-Y., Guo, G., Wang, P., ZHANG, W., Fei, Z., Zhen, H.-N., You, S.-W., and Yang, H. (2009). Brain Tumor Stem-Like Cells Identified by Neural Stem Cell Marker CD15. Transl Oncol 2, 247–257.

Morrison, S.J., and Kimble, J. (2006). Asymmetric and symmetric stem-cell divisions in development and cancer. Nature 441, 1068–1074.

Nicolaides, T.P., Li, H., Solomon, D.A., Hariono, S., Hashizume, R., Barkovich, K., Baker, S.J., Paugh, B.S., Jones, C., Forshew, T., et al. (2011). Targeted Therapy for BRAFV600E Malignant Astrocytoma. Clin. Cancer Res. 17, 7595–7604.

Noctor, S.C., Martínez-Cerdeño, V., Ivic, L., and Kriegstein, A.R. (2004). Cortical neurons arise in symmetric and asymmetric division zones and migrate through specific phases. Nat. Neurosci. 7, 136–144.

Oda, K., Matsuoka, Y., Funahashi, A., and Kitano, H. (2005). A comprehensive pathway map of epidermal growth factor receptor signaling. Mol. Syst. Biol. 1, 2005.0010.

Persson, A.I., Petritsch, C., Swartling, F.J., Itsara, M., Sim, F.J., Auvergne, R., Goldenberg, D.D., Vandenberg, S.R., Nguyen, K.N., Yakovenko, S., et al. (2010). Non-stem cell origin for oligodendroglioma. Cancer Cell 18, 669–682.

Peyssonnaux, C., Provot, S., Felder-Schmittbuhl, M.P., Calothy, G., and Eychène, A. (2000). Induction of postmitotic neuroretina cell proliferation by distinct Ras downstream signaling pathways. Mol. Cell. Biol. 20, 7068–7079.

Prados, M.D., Chang, S.M., Butowski, N., DeBoer, R., Parvataneni, R., Carliner, H., Kabuubi, P., Ayers-Ringler, J., Rabbitt, J., Page, M., et al. (2009). Phase II study of erlotinib plus temozolomide during and after radiation therapy in patients with newly diagnosed glioblastoma multiforme or gliosarcoma. J. Clin. Oncol. 27, 579–584.

Pritchard, C.A., Bolin, L., Slattery, R., Murray, R., and McMahon, M. (1996). Post-natal lethality and neurological and gastrointestinal defects in mice with targeted disruption of the A-Raf protein kinase gene. Curr. Biol. 6, 614–617.

Raabe, E.H., Lim, K.S., Kim, J.M., Meeker, A., Mao, X.-G., Nikkhah, G., Maciaczyk, J., Kahlert, U., Jain, D., Bar, E., et al. (2011). BRAF activation induces transformation and then senescence in human neural stem cells: a pilocytic astrocytoma model. Clin. Cancer Res. 17, 3590–3599.

Raponi, E., Agenes, F., Delphin, C., Assard, N., Baudier, J., Legraverend, C., and Deloulme, J.C. (2007). S100B expression defines a state in which GFAP-expressing cells lose their neural stem cell potential and acquire a more mature developmental stage. Glia 55, 165–177.

Reynolds, B.A., and Weiss, S. (1992). Generation of neurons and astrocytes from isolated cells of the adult mammalian central nervous system. Science 255, 1707–1710.

Rhyu, M.S., Jan, L.Y., and Jan, Y.N. (1994). Asymmetric distribution of numb protein during division of the sensory organ precursor cell confers distinct fates to daughter cells. Cell 76, 477–491.

Rodriguez, E.F., Scheithauer, B.W., Giannini, C., Rynearson, A., Cen, L., Hoesley, B., Gilmer-Flynn, H., Sarkaria, J.N., Jenkins, S., Long, J., et al. (2011). PI3K/AKT pathway alterations are associated with clinically aggressive and histologically anaplastic subsets of pilocytic astrocytoma. Acta Neuropathol. 121, 407–420.

Rolls, M.M., Albertson, R., Shih, H.-P., Lee, C.-Y., and Doe, C.Q. (2003). Drosophila aPKC regulates cell polarity and cell proliferation in neuroblasts and epithelia. J. Cell Biol. 163, 1089–1098.

Sala, E., Mologni, L., Truffa, S., Gaetano, C., Bollag, G.E., and Gambacorti-Passerini, C.

(2008). BRAF silencing by short hairpin RNA or chemical blockade by PLX4032 leads to different responses in melanoma and thyroid carcinoma cells. Mol. Cancer Res. 6, 751–759.

Salomon, D.S., Brandt, R., Ciardiello, F., and Normanno, N. (1995). Epidermal growth factor-related peptides and their receptors in human malignancies. Crit. Rev. Oncol. Hematol. 19, 183–232.

Schaefer, M., Petronczki, M., Dorner, D., Forte, M., and Knoblich, J.A. (2001). Heterotrimeric G proteins direct two modes of asymmetric cell division in the Drosophila nervous system. Cell 107, 183–194.

Schiffman, J.D., Hodgson, J.G., Vandenberg, S.R., Flaherty, P., Polley, M.-Y.C., Yu, M., Fisher, P.G., Rowitch, D.H., Ford, J.M., Berger, M.S., et al. (2010). Oncogenic BRAF mutation with CDKN2A inactivation is characteristic of a subset of pediatric malignant astrocytomas. Cancer Res. 70, 512–519.

Schindler, G., Capper, D., Meyer, J., Janzarik, W., Omran, H., Herold-Mende, C., Schmieder, K., Wesseling, P., Mawrin, C., Hasselblatt, M., et al. (2011). Analysis of BRAF V600E mutation in 1,320 nervous system tumors reveals high mutation frequencies in pleomorphic xanthoastrocytoma, ganglioglioma and extra-cerebellar pilocytic astrocytoma. Acta Neuropathol. 121, 397–405.

Schwartz, P.H., Brick, D.J., Stover, A.E., Loring, J.F., and Müller, F.-J. (2008). Differentiation of neural lineage cells from human pluripotent stem cells. Methods 45, 142–158.

Seaberg, R.M., and van der Kooy, D. (2003). Stem and progenitor cells: the premature desertion of rigorous definitions. Trends in Neurosciences 26, 125–131.

Setoguchi, T., and Kondo, T. (2004). Nuclear export of OLIG2 in neural stem cells is essential for ciliary neurotrophic factor-induced astrocyte differentiation. J. Cell Biol. 166, 963–968.

Shen, Q., Zhong, W., Jan, Y.N., and Temple, S. (2002). Asymmetric Numb distribution is critical for asymmetric cell division of mouse cerebral cortical stem cells and neuroblasts. Development 129, 4843–4853.

Siegel, R., Naishadham, D., and Jemal, A. (2013). Cancer statistics, 2013. CA Cancer J Clin 63, 11–30.

Silber, J., Lim, D.A., Petritsch, C., Persson, A.I., Maunakea, A.K., Yu, M., Vandenberg, S.R., Ginzinger, D.G., James, C.D., Costello, J.F., et al. (2008). miR-124 and miR-137 inhibit proliferation of glioblastoma multiforme cells and induce differentiation of brain tumor stem cells. BMC Med 6, 14.

Siller, K.H., Cabernard, C., and Doe, C.Q. (2006). The NuMA-related Mud protein binds Pins and regulates spindle orientation in Drosophila neuroblasts. Nat. Cell Biol. 8, 594–600.

Son, M.J., Woolard, K., Nam, D.-H., Lee, J., and Fine, H.A. (2009). SSEA-1 is an enrichment marker for tumor-initiating cells in human glioblastoma. Cell Stem Cell 4, 440–452.

Sugiarto, S., Persson, A.I., Munoz, E.G., Waldhuber, M., Lamagna, C., Andor, N., Hanecker, P., Ayers-Ringler, J., Phillips, J., Siu, J., et al. (2011). Asymmetry-Defective Oligodendrocyte Progenitors Are Glioma Precursors. Cancer Cell 20, 328–340.

Sun, Y., Goderie, S.K., and Temple, S. (2005). Asymmetric distribution of EGFR receptor during mitosis generates diverse CNS progenitor cells. Neuron 45, 873–886.

Tajbakhsh, S., Rocheteau, P., and Le Roux, I. (2009). Asymmetric cell divisions and asymmetric cell fates. Annu. Rev. Cell Dev. Biol. 25, 671–699.

Takebayashi, H., Nabeshima, Y., Yoshida, S., Chisaka, O., Ikenaka, K., and Nabeshima, Y.-I. (2002). The basic helix-loop-helix factor olig2 is essential for the development of motoneuron and oligodendrocyte lineages. Curr. Biol. 12, 1157–1163.

Tsai, J., Lee, J.T., Wang, W., Zhang, J., Cho, H., Mamo, S., Bremer, R., Gillette, S., Kong, J., Haass, N.K., et al. (2008). Discovery of a selective inhibitor of oncogenic B-Raf kinase with potent antimelanoma activity. Proc. Natl. Acad. Sci. U.S.a. 105, 3041–3046.

Van Aelst, L., Barr, M., Marcus, S., Polverino, A., and Wigler, M. (1993). Complex formation between RAS and RAF and other protein kinases. Proc. Natl. Acad. Sci. U.S.a. 90, 6213–6217.

Verhaak, R.G.W., Hoadley, K.A., Purdom, E., Wang, V., Qi, Y., Wilkerson, M.D., Miller, C.R., Ding, L., Golub, T., Mesirov, J.P., et al. (2010). Integrated genomic analysis identifies clinically relevant subtypes of glioblastoma characterized by abnormalities in PDGFRA, IDH1, EGFR, and NF1. Cancer Cell 17, 98–110.

Wang, Y., Yang, J., Zheng, H., Tomasek, G.J., Zhang, P., McKeever, P.E., Lee, E.Y.-H.P., and Zhu, Y. (2009). Expression of mutant p53 proteins implicates a lineage relationship between neural stem cells and malignant astrocytic glioma in a murine model. Cancer Cell 15, 514–526.

Watt, F.M., and Hogan, B.L. (2000). Out of Eden: stem cells and their niches. Science 287, 1427–1430.

Weiss, S., Reynolds, B.A., Vescovi, A.L., Morshead, C., Craig, C.G., and van der Kooy, D. (1996). Is there a neural stem cell in the mammalian forebrain? Trends in Neurosciences 19, 387–393.

Weiss, W.A., Burns, M.J., Hackett, C., Aldape, K., Hill, J.R., Kuriyama, H., Kuriyama, N., Milshteyn, N., Roberts, T., Wendland, M.F., et al. (2003). Genetic determinants of malignancy in a mouse model for oligodendroglioma. Cancer Res. 63, 1589–1595.

Weissman, I.L. (2000). Stem cells: units of development, units of regeneration, and units in evolution. Cell 100, 157–168.

Wick, W., Weller, M., Weiler, M., Batchelor, T., Yung, A.W.K., and Platten, M. (2011). Pathway inhibition: emerging molecular targets for treating glioblastoma. Neuro-Oncology 13, 566–579.

Wirtz-Peitz, F., Nishimura, T., and Knoblich, J.A. (2008). Linking cell cycle to asymmetric

division: Aurora-A phosphorylates the Par complex to regulate Numb localization. Cell 135, 161–173.

Yuan, S.H., Martin, J., Elia, J., Flippin, J., Paramban, R.I., Hefferan, M.P., Vidal, J.G., Mu, Y., Killian, R.L., Israel, M.A., et al. (2011). Cell-surface marker signatures for the isolation of neural stem cells, glia and neurons derived from human pluripotent stem cells. PLoS ONE 6, e17540.

Zebisch, A., and Troppmair, J. (2006). Back to the roots: the remarkable RAF oncogene story. Cell Mol Life Sci 63, 1314–1330.

7 Curriculum Vitae – Brian Reichholf

Research Interests

Molecular Biology: ncRNA in development, RNA localisation, translational kinetics
IT & Engineering: pathfinding algorithms, microfluidics, labs-on-a-chip

Education

University of Vienna

M.Sc., Molecular Cell Biology **2013**
B.Sc., Molecular Biology **2011**

Graduation from technical college (electronics & network engineering) **2003**

Academic Experience

University of California, San Francisco – Master Thesis **Nov 2011 to Nov 2012**

Department of Neurological Surgery – Petritsch Lab
Researching the function of the BRafV600E mutation in adult neural stem cells and paediatric malignant astrocytomas for my master's thesis, predominantly using cell culture based assays to elucidate the role of BRafV600E on differentiation, proliferation and asymmetric cell division.

University of Veterinary Medicine, Vienna – Lab rotation **Aug and Sep 2011**

Institute of Pharmacology and Toxicology – Sexl Lab.
Researching the role of Stat3 in NK-cell mediated tumour surveillance during a two-month lab rotation, using tissue and cells harvested from mice and performing flow cytometry and western blot analysis.

University of Vienna

- Tutor for an undergraduate molecular biology lab **since Feb 2011**
  Assisting undergraduates in setting up experiments for plasmid transfection, DNA extraction, bacterial culturing, PCR, gel electrophoretic analysis, restriction analysis, cloning and x-gal staining. Ensuring proper understanding of the required concepts, mathematical and chemical knowledge.
- Mentor for first year students **Oct 2010 to Feb 2011**
  Guiding students through university and ensuring a smooth transition from college/high school to university. Helping them settle in to university life; establish a decent learning rhythm; provide answers to questions about stipends, housing and student rights.
- Bachelor Thesis, Max F. Perutz Laboratories **Apr to June 2010**
  Department of Biochemistry and Cell Biology – Wiche Lab.
  Researching the role of plectin in vascular endothelial cells using western blot analysis, co-immunoprecipitation and histological analysis.

Professional Experience

Vienna Open Lab – Tutor **since June 2011**

Teaching basic scientific concepts (e.g. different states of matter; surface tension; and hydrophobic vs hydrophillic – ages 5-7), biology (e.g. DNA extraction from plants or oral mucosa – ages 10-14) and molecular biology (e.g. influence of genes on sleep; analysis of meat to determine content of beef, pork, goat and horse meat – ages 16 and up) establishing the required theoretic understanding and performing according experiments such as DNA extraction, enzymatic restriction, PCR and gel electrophoresis.

Cochlear, Hannover – Clinical Technical Specialist **2005 to 2007**

Arbeiter Samariter Bund Österreich – Emergency Care Assistant **2004 to 2005**

Login GmbH – Network and System Administrator **2003**

Wet Lab Skills

Mouse work

- Husbandry; genotyping; ear-notching; dissection and isolation of cells from various tissues including brain, liver, spleen and intra-femural bone marrow
- Subcutaneous, intracranial and intraperitoneal injections

Cell culture work

- Developed a novel method to compare enzymatic expression using immunofluorescent staining and semi-automated scripted analysis in ImageJ.
- Established a novel method to compare growth speed and drug dosage effects on proliferation across cell lines using alamarBlue.
- Set up a protocol for crude expression comparison of genes in cell lines.
- Culturing and handling of: primary cells; cell lines; neural and embryonic stem cells; and viral infections of all of the above.

IT Skills

Text processing: LaTeX, Excel, PowerPoint, Word
Image processing: Adobe Photoshop, InDesign, Illustrator, ImageJ
Web & Programming: HTML, PHP, Python, Bash and Perl scripting
Miscellaneous: Linux server maintenance, Windows, Mac and Linux first level support

Publications

Divergent effects of BRaf^{V600E} in distinct populations of neural stem and progenitor cells contribute to tumorigenesis and therapy response., R. Lerner, Y. Ihara, A. Griveau, D. Qu, T. Ozawa, B. Reichholf, R.A. Ihrie, S. Sugiarto, J.J. Phillips, M. McMahon, D.H. Rowitch, D.C. James, C. Petritsch (in preparation)
Transformational effects of BRaf^{V600E} in neural stem and progenitor cells, B. Reichholf, S. Sugiarto, N. Andor, M. McMahon, D.C. James and C. Petritsch, Tri-Institutional Stem Cell Retreat, 11-13 April 2012 (poster)